RIASSUNTO

La sindrome genetica rara da disabilità intellettiva e disturbo del ritmo cardiaco (acronimo: IDDCA, MIM # 617173) è una malattia multi-sistemica a trasmissione autosomica recessiva con esordio precoce, associata a varianti patogenetiche nel gene *GNB5*. Il quadro delle manifestazioni cliniche varia da una forma più grave caratterizzata da ritardo nello sviluppo psicomotorio, disabilità intellettiva, encefalopatia epilettica, anomalie visive e aritmie cardiache (IDDCA), a una forma più lieve associata al ritardo del linguaggio, disturbo da deficit di attenzione, deficit cognitivo, in presenza o assenza di aritmia cardiaca (LADCI). Trattandosi di una sindrome rara, pochi casi sono stati descritti in tutto il mondo, di cui l'ottanta per cento caratterizzati da aritmia cardiaca. Sebbene sia stata stabilita la causa genetica della sindrome, non è ancora chiaro il meccanismo alla base della malattia, rendendo più difficile lo sviluppo di trattamenti mirati per una possibile terapia.

Il gene GNB5 codifica per Gβ5, un membro che diverge dalle altre sub-unità beta della famiglia delle proteine G eterotrimeriche. Caratteristica peculiare della proteina GNB5 è la sua capacità di formare complessi proteici con i membri del gruppo R7 dei regolatori della segnalazione cellulare mediata dalle proteine G (R7-RGS), con i quali GNB5 esercita un effetto di regolazione negativa sulla segnalazione cellulare mediata dall'attività dei recettori accoppiati alle proteine G (GPCR), inibendo il rilascio di diversi neurotrasmettitori implicati nell'apprendimento, nel controllo motorio oltre che nella vista.

Le peculiari manifestazioni cliniche riscontrate nei pazienti affetti dalla sindrome da IDDCA, riconducibili a convulsioni epilettiche, disabilità intellettiva e bradicardia, possono essere attribuite ad alterazioni dell'eccitabilità cellulare poiché GNB5, insieme al gruppo delle proteine R7-RGS, è un membro cruciale nella modulazione della cinetica di attivazione dei canali del potassio attivati dalle proteine G (GIRK) e di altri canali ionici, implicati nella regolazione della funzione neuronale e cardiaca. Questo è supportato dai dati riportati in letteratura, che identificano GNB5 come parte di un complesso multi-proteico composto da GPCR/GNB5/R7-RGS/GIRK. La nostra ipotesi progettuale è che le principali manifestazioni riscontrate nei pazienti siano causate principalmente dalla destabilizzazione di tali complessi proteici, con conseguente alterazione dell'eccitabilità cellulare.

Nel nostro studio dimostriamo come il segnale cellulare mediato dalla proteina GNB5 sia essenziale per il controllo del sistema parasimpatico sulla frequenza cardiaca. Nello specifico, abbiamo ingegnerizzato cellule staminali pluripotenti indotte (hiPSC), in cui abbiamo rimosso il gene GNB5 (hiPSC), sottoposte in seguito al differenziamento cellulare in senso cardiogenico. I nostri risultati preliminari ottenuti dai cardiomiociti derivati dalle linee cellulari di hiPSCKO (iCMKO), mostrano

una frequenza cardiaca alterata caratterizzata da una spiccata bradicardia se confrontata con quella dei cardiomiociti di controllo (iCMWT). È interessante notare che, in accordo con l'ipotesi di ipersensibilità muscarinica, l'applicazione di un antagonista dei recettori muscarinici cardiaci o di un bloccante dei canali GIRK, in parte favoriscano un recupero del fenotipo bradicardico associato all'assenza della proteina GNB5. Questi risultati indicano che il nostro modello cellulare "*in vitro*" è efficace per approfondire le conoscenze sui meccanismi molecolari alla base della sindrome da IDDCA e che pertanto potrebbe essere un buon modello per testare e identificare nuove molecole da utilizzare come punto di partenza per la sperimentazione di un programma finalizzato a una possibile terapia.


Università di Foggia

**UNIVERSITÀ DEGLI STUDI DI FOGGIA**

**FACULTY OF MEDICINE AND SURGERY**

PhD Course in Experimental and Regenerative Medicine
XXXI Cycle

# *Dissecting the IDDCA (Intellectual Developmental Disorder with Cardiac Arrhythmia) syndrome pathogenic mechanisms*

***Tutor***
*Prof. V.M Fazio*

***PhD Student***
*Natascia Malerba*

***Supervisor***
*Dr. Giuseppe Merla*

---

A.A. 2017/2018

**INDEX**

**ABSTRACT**

Homozygous and compound heterozygous pathogenic variants in *GNB5* have been recently associated with a spectrum of clinical presentations varying from a severe multisystem form of the disorder including intellectual disability, early infantile developmental and epileptic encephalopathy, retinal abnormalities and cardiac arrhythmias (IDDCA) to a milder form with language delay, attention-deficit/hyperactivity disorder, cognitive impairment, with or without cardiac arrhythmia (LADCI). Very few affected patients have been described worldwide with ~80% of them having cardiac arrhythmia. Although genetic cause of IDDCA has been established, we have a poor understanding of the disease mechanism and are thus unable to work towards developing targeted treatments for this devastating syndrome. The GNB5 gene encodes for Gβ5, a divergent member of the beta subunits of heterotrimeric G proteins. A unique hallmark of GNB5 is its ability to form complexes with members of the R7 group of regulators of G-protein signalling (R7-RGS), that serve as negative regulators of GPCR signalling, inhibiting the release of several neurotransmitters implicated in learning, motor control, and vision, among others. Based on the IDDCA patient's symptoms, epileptic encephalopathy/seizures, cognitive impairment, and bradycardia can be attributed to alterations in cell excitability and, indeed, GNB5, together with R7-RGS proteins, is a crucial player of the GPCR cascade, including neuronal and cardiac signalling mediated by GIRK and other ion channels. Supporting this, GNB5 has been recently identified as part of a protein complex composed of GPCR/GNB5/R7-RGS/GIRK. We hypothesize that the prominent cardiac manifestation of IDDCA is caused mainly by destabilization of such complexes resulting in impaired cell excitability.

Here we show that *GNB5* signaling is essential for parasympathetic control of heart rate. Specifically, we engineered human induced pluripotent stem cells (hiPSCs) knocked-out for *GNB5* (hiPSCKO) that was subjected to cardiogenic differentiation. Our preliminary results show that hiPSCKO-derived cardyomyocites (iCMKO) exhibit altered heart rate with marked bradycardia when compared to control cardyomyocytes (iCMWT). Interestingly, and in agreement with the hypothesis of muscarinic hypersensitivity, application of a muscarinic antagonist, or GIRK channels blocker, partially rescue the bradycadic phenotype associated with GNB5 KO.

These results indicate that our cellular models are "*in vitro"* effective models to deeper our knowledge about the molecular mechanisms of IDDCA syndrome, and could be used to test and identify some candidate molecules for further therapeutic approaches or as a starting point for drug optimization program

# INTRODUCTION

## Human Induced Pluripotent Stem Cells (hiPSCs)

In 2006, Takahashi and Yamanaka demonstrated the possibility to reprogram the fate of both murine and human somatic cells bringing them back to a pluripotent state. They showed that four exogenous reprogramming factors, including Oct 3/4 (Octamer-binding transcription factor-3/4), Sox2 (Sex-determining region Y)-box 2, Klf4 (Kruppel Like Factor-4), and c-Myc nicknamed the "OSKM factors", all have key roles in human induced pluripotent stem cells (hiPSC) generation. These factors are pluripotency-associated genes expressed early during embryonic development and are involved in the maintenance of pluripotency and self-renewal (Takahashi and Yamanaka, 2006; Takahashi et al., 2007). Prior to the discovery of hiPSCs, human embryonic stem cells (hESCs), derived from the inner cell mass (ICM) of a blastocyst of pre-implantation stage embryo, was the most well-known pluripotent stem cells. However, broad application on hESCs remains challenging due to the technical difficulties like immune rejection after transplantation of non-autologous cells and ethical concerns associated with the use of human embryos for research (Soldner and Jaenisch, 2018). The hiPSCs - defined as "embryonic stem cell-like" - have a self-renewal capability in culture, can differentiate into cell types from all three germ cell layers (ectoderm, mesoderm, and endoderm), and resolves many limitations associated with the use of hESCs.

The strength of this technology resides in the possibility to obtain large quantities of cells from patients carrying a specific genetic background, including those alterations responsible for the pathology and is particularly crucial for those diseases for which we face with the impossibility to access the diseases-relevant human tissues. The hiPSCs can proliferate extensively in culture and differentiate into all types of cells of the human body, thus recapitulating the "human disease in a Petri dish" (Figure 1).

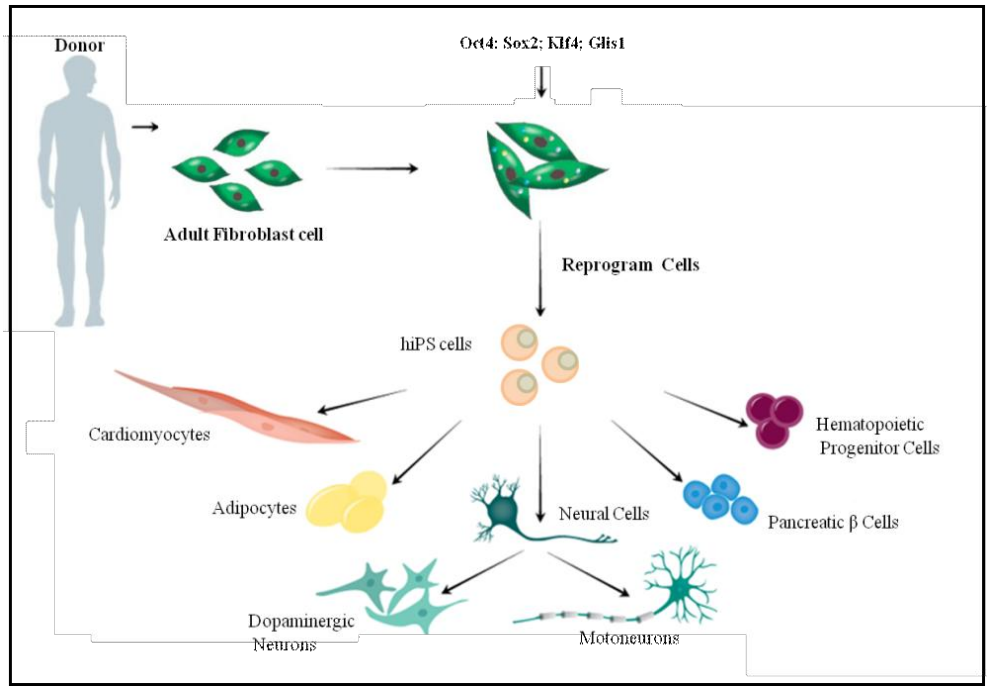


**Figure 1.** Generation of hiPSCs from skin fibroblast cultures and their ability to differentiate in different cell types.

Derivation of hiPSC from somatic cells (Takahashi et al., 2007) has generated significant enthusiasm for its potential application in basic and translational research, since they carry the same genome as the patient they were generated from, and offer the opportunity to generate disease-specific and patient specific hiPSCs for modeling human diseases, drug development and screening, and individualized regenerative cell therapy (Omole and Fakoya, 2018). Moreover, its current combination with genome editing by CRISPR/Cas9 has further enhanced the diagnostic and therapeutic power of the hiPSCs (Hotta and Yamanaka, 2015). Their application in regenerative medicine allows us to improve our knowledge of human genetic diseases, for which a therapy is not available yet.

## G-Protein Coupled Receptors (GPCRs)

G-protein-coupled receptors (GPCRs) are the largest group of cell-surface seven-transmembrane proteins (TM) (Kamato et al., 2013) which has a ligand-binding pocket in the extracellular region, the TM region which contains seven TM α-helices, and a cytoplasmic interacting region (Pierce et al., 2002; Lagerstrom and Schioth, 2008) to mediate intracellular signalling crucial for neuronal communication, including regulation of the antagonistic effects of the parasympathetic and sympathetic branches of the autonomic nervous system throughout the body. GPCRs are encoded by nearly 800 different genes in the human genome and represent the largest TM receptors family found in humans (Bockaert and Pin, 1999). There are five subclasses of receptors on the bases of their sequences and structural

similarities, rhodopsin (class A), secretin (class B), glutamate (class C), adhesion and Frizzled/Taste2 (reviewed in (Zhao et al., 2016)). GPCRs transduce different extracellular stimuli by activating different isoform of G proteins (Gs, $Gq/_{11}$, Gi, $G_{12/13}$), which promote different signalling cascades inside cells (Azzi et al., 2003; Fredriksson et al., 2003; Rosenbaum et al., 2009; Rajagopal et al., 2010).

G-proteins exist as heterotrimeric complex composed of three subunits, a guanine-nucleotide binding α-subunit (Gα) with GTPase activity and a tight dimer consisting of β and γ subunits (Gβγ) (Gilman, 1987; Morris and Malbon, 1999; McCudden et al., 2005). The combinatorial association of the different G protein subunits, composed of at least 20 different Gα, 6 different Gβ (including the two isoforms Gβ5 and Gβ5L), and 13 different Gγ subunits (Watson et al., 1996; Vincent et al., 2016) provides the level of selectivity that is needed to generate the wide range of signals activated by G proteins (Robishaw and Berlot, 2004; Dupre et al., 2009; Khan et al., 2013) in modulating many important cellular functions, including the release of hormones and growth factors, the regulation of cell contraction and migration, as well as cell growth and differentiation (Trivellin et al., 2014; Krishnan et al., 2015; Trivellin et al., 2016). Ligand binding of a GPCR acts as guanine-nucleotide exchange factors (GEFs) that promote a GPCR conformational change that then activates trimeric G-proteins by promoting the exchange of GDP to GTP on the Gα subunit, and its dissociation from Gβγ dimer. Both Gα-GTP and Gβγ subunits modulate downstream intracellular signalling by interacting with specific effector proteins (Figure 2) (Gilman, 1987; Neer, 1995; Clapham and Neer, 1997; Cabrera-Vera et al., 2003; Smrcka, 2008; Vilardaga et al., 2010).

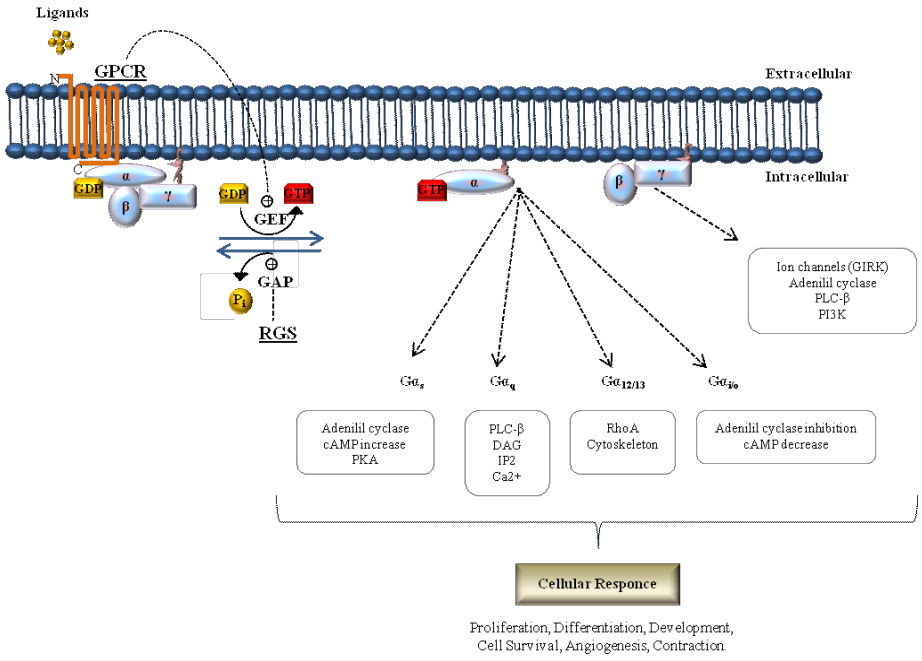


**Figure 2.** Model of GPCR mediated signalling pathways.

**Regulator of G-protein signaling (RGS)**

The propagation of the GPCR cascades is controlled by the action of the regulators of G protein signalling (RGS). The regulator of RGS acts limiting the active Gα species lifetime by their GTPase activating (GAP) function, accelerating Gα GTP hydrolysis and thus resulting in a response deactivation of GPCRs-initiated signalling and its re-association with Gβγ dimer (Neer, 1995; Berman et al., 1996; Hunt et al., 1996; Watson et al., 1996; Hepler et al., 1997; Kozasa et al., 1998; De Vries et al., 2000). The RGS proteins are encoded by more than 30 genes in mammals and have been classified into six subfamilies (Anderson et al., 2009; Aguado et al., 2016). Specifically, the R7 group of RGS (R7-RGS) include four highly homologous mammalian proteins namely RGS6, RGS7, RGS9, RGS11 (Sondek and Siderovski, 2001; Xie et al., 2010) which are highly expressed in neurons (Gold et al., 1997).

Like other members of the larger RGS protein family, R7-RGS proteins contain i) a C-terminal core RGS homology domain that act as GTPase activating protein (GAP) (Ross and Wilkie, 2000); ii) the N-terminal Disheveled, EGL-10, Pleckstrin (DEP) and DEP helical extension (DHEX) protein domains, that are essential for protein-protein interactions critical for plasma membrane anchors (Tayou et al., 2016); and iii) the centrally located domain referred to as a Gγ-like (GGL) domain, which is responsible for the direct interaction with the divergent Gβ subunit, Gβ5 (Tayou et al., 2016).

**G-protein beta subunits**

G-proteins exist as heterotrimeric complex composed of three subunits, α, β, and γ (Gβγ) (Gilman, 1987; Morris and Malbon, 1999; McCudden et al., 2005). The G protein beta subunits (Gβ) belong to the beta-propeller family of proteins characterized by seven regular WD-40 repeats (WD-40) and a coiled coil domain at the far end N-terminus. The WD40 (also known as WD or beta-transducin repeats) domain is one of the most abundant and interacting domains in the eukaryotic genome; each of them is approximately 40 amino acids long and is characterized by a conserved tryptophan (Trp; W) -aspartic (Asp; D) acid pair, from which the WD40 domain is named (Watson et al., 1994; Sondek et al., 1996). In proteins the WD repeats folds into a β-propeller architecture, providing a platform for protein–protein or protein–DNA interaction, and to coordinate downstream cellular events including signal transduction, autophagy, and apoptosis (Neer et al., 1994; Jain and Pandey, 2018). The coiled-coil domain involving α-helical segments at the N termini of the β and γ subunits and contributes in βγ dimerization and effector signalling (Pellegrino et al., 1997).

In humans five different Gβ subunits, encoded by *GNB1* to *GNB5* genes have been identified. The first four Gβ1-4 subunits share between 80 and 90% sequence identity while Gβ5 shares

only 50% of sequence homology with the other four members, and is the only one that can have cellular other than cell membrane localization (Fletcher et al., 1998).

**G protein subunit beta 5 (GNB5)**

The *GNB5* gene (MIM 604447), (NM_006578; located at 15q21.2 chromosome region) encodes for Gβ5 subunit of the heterotrimeric G-protein complex and encodes for a protein of 353 amino acid residues with 11 coding exons. GNB5 is broadly expressed in neural, neuroendocrine and other excitable tissue such as heart muscle (Slepak, 2009; Posokhova et al., 2010) with an additional longer Gβ5 isoform (Gβ5L) that is expressed in the vertebrate retina photoreceptors (Watson et al., 1994; Watson et al., 1996; Gautam et al., 1998; Robishaw and Berlot, 2004; McCudden et al., 2005).

The Gβ5 is a divergent member of the Gβ family which exhibits distinct biochemical properties respect to other members (Fletcher et al., 1998). Recent evidence suggests the existence of supramolecular complexes with members of the R7 group of regulators of G-protein signalling (R7-RGS). The obligatory interaction between Gβ5 and R7-RGS, by the GGL domain, is required for their mutual stability, indeed without their partner, both proteins are rapidly degraded in cells (Chen et al., 2000; Simonds and Zhang, 2000; Martemyanov et al., 2005). Consistently, in knockout mouse studies, the genetic ablation of the *Gnb5* resulted in the instability of all R7-RGS proteins (Chen et al., 2003). GNB5 has an unusual selectivity for its effectors, as it potently regulates the activities of PLC β2, N-type calcium channels, and G protein-coupled inwardly-rectifying potassium (GIRK) channels (Watson et al., 1994; Yoshikawa et al., 2000).

**G protein-gated K+ channels (GIRK)**

G protein-coupled inwardly-rectifying potassium (GIRK) (Kir3) channels are important transducers of inhibitory neurotransmitter effects in heart and brain. They regulate heartbeat, neuronal excitability and plasticity, analgesia, alcohol and drug effects, and are implicated in a number of disorders such as epilepsy, Down syndrome, bipolar disorder, atrial fibrillation and primary aldosteronism (Yakubovich et al., 2015; Chen et al., 2017).

The GIRK family has four members: Kir3.1 (GIRK1), Kir3.2 (GIRK2), Kir3.3 (GIRK3) and Kir3.4 (GIRK4). Most of the GIRK channels are heterotetramers in native tissues, especially Kir3.1–Kir 3.2 in the brain and Kir3.1–Kir 3.4 in the heart, control the excitability of neurons and the heart rate, respectively (Noma and Trautwein, 1978; Kubo et al., 1993; Lesage et al., 1994; Hibino et al., 2010). GIRK channels are directly activated by Gβγ subunits when $G_{i/o}$ coupled GPCR on the membrane of the same cell is activated by agonists, which results in the

dissociation of Gβγ from Gα. As a consequence of GIRK channels activation, the corresponding outward potassium ($K^+$) current moves the membrane potential to a more hyperpolarized potential, far from the firing threshold therefore delaying the triggering of the next action potential (Yoshikawa et al., 2000; Yakubovich et al., 2015).

**R7-RGS/GNB5 Complex**

In hippocampal CA1 pyramidal neurons, R7-RGS/GNB5 forms macromolecular complexes with the $GABA_B$ receptors ($GABA_BR$) and the G protein-coupled inwardly-rectifying potassium (GIRK) channels (Fajardo-Serrano et al., 2013). For instance, co-expression of R7-RGS/GNB5 with the anchoring protein R7BP enhances the ability of RGS7 to increase muscarinic M2 receptor-dependent GIRK channel activation, presumably due to the stimulation of the catalytic activity of RGS7 (Yang et al., 2010; Zhou et al., 2012). The activation of postsynaptic $GABA_BR$ on pyramidal neurons produces slow inhibitory postsynaptic currents (sIPSCs), which counteract the excitatory influence of ionotropic glutamate receptors to shape neuronal output (Ulrich and Bettler, 2007; Luscher and Slesinger, 2010). As a result, $GABA_BR$ signalling profoundly affects hippocampal synaptic plasticity and has marked effects on memory formation (Davies et al., 1991; Schuler et al., 2001; Ostrovskaya et al., 2014). Most of the postsynaptic inhibitory effect of $GABA_BR$ stimulation in the hippocampus is mediated by activation GIRK channels; which inhibit neuronal excitability via hyperpolarizing K+ efflux (Luscher and Slesinger, 2010). Blockade of $GABA_BR$ or GIRK channels by either pharmacological manipulations or genetic knockout ablates the slow IPSC, and blunts a form of hippocampal synaptic plasticity known as depotentiation (Chung et al., 2010). In hippocampal pyramidal neurons, $GABA_BR$-GIRK signalling is negatively modulated by RGS7-Gβ5-R7BP complex. RGS7 is closely co-localized with both $GABA_BR$ and GIRK2-containing channels (Fajardo-Serrano et al., 2013). Moreover the interaction between RGS7 with GIRK channels is mediated by Gβ5 subunit and is facilitated by R7BP, to limit the duration of GIRK activity evoked by $GABA_BR$ in hippocampal neurons (Zhou et al., 2012). Given the established role of $GABA_B$ receptors and GIRK channels in many neurological diseases (Lujan and Ciruela, 2012; Lujan et al., 2014), the regulation of GNB5 is likely crucial in such pathologies..

As in neurons, the R7-RGS/GNB5 complex negatively regulates the GIRK channels also in cardiomyocytes (Posokhova et al., 2010). Cardiac rate is controlled by the sympathetic and parasympathetic branches of the autonomic nervous system. In the sinus node, the

parasympathetic modulation of cardiac output is mediated primarily by acetylcholine (ACh) release from the vagus nerve which binds and activates the muscarinic receptor ($M_2R$).

The activation of $M_2R$ triggers the release of inhibitory G proteins, activates the potassium current $I_{KACh}$ by GIRK channels ($M_2R$-$I_{KACh}$); that hyperpolarize the membrane potential far from the firing threshold thus slowing action potential rate. Activation of $M_2R$ associated G proteins also inhibits the adenylyl cyclase (AC) activity. AC inhibition causes a decrease in the intracellular concentration of cAMP, a decrease in f-channels (HCN) activity and consequently a slower rate of the sinus node (DiFrancesco et al., 1989; DiFrancesco, 2010; Yang et al., 2010). All of these ionic mechanisms are thus potentially involved in the cholinergic regulation of heart rate (Mangoni and Nargeot, 2008).

In cardiac tissue, the $M_2R$-$I_{KACh}$ signalling is negatively regulated by RGS6 which is implicated in modulation of parasymphatetic stimulation of the heart. In particular, a specific interaction of the Gβ5 and RGS6 - via the GGL domain - prominently accelerate $I_{KACh}$ deactivation kinetics in sinoatrial nodal cells and cardiac myocytes (Kulkarni et al., 2018) functioning to prevent parasymphathetic override and severe bradycardia (Yang et al., 2010). The physical association between RGS6 and Gβ5 is critical for their expression and/or stability (Posokhova et al., 2010). RGS6-GNB5 involvement in $M_2R$-$I_{KACh}$ signalling is mediated by a direct protein-protein interaction with the cardiac-specific GIRK subunit, GIRK4 (Posokhova et al., 2010), suggesting that the association of RGS6-GNB5-$I_{KACh}$ also plays critical role in controlling heart rate.

**G-protein β subunits and Human Genetic Diseases**

In human pathogenic variants in each of the five distinct G proteins β-subunits, encoded by the *GNB1-GNB5* genes, cause genetic disorders with variable brain and heart involvement. Germline *de novo GNB1* variants cause severe neurodevelopmental disability, hypotonia, and seizures (Petrovski et al., 2016); *GNB3* bi-allelic loss-of-function (LoF) variants has been linked to congenital stationary night blindness (Vincent et al., 2016), recessive retinopathy in human (Arno et al., 2016) retinal degeneration in chicken (Tummala et al., 2006) and a reduced cone sensitivity with bradycardia in mice (Nikonov et al., 2013; Ye et al., 2014). A single nucleotide polymorphism (SNP) in *GNB3* was associated with postural tachycardia syndrome (Nakao et al., 2012), incidence of cardiovascular disease and stroke (Zhang et al., 2005). *GNB2* pathogenic variants cause sinus node and atrioventricular conduction dysfunction (Stallmeyer et al., 2017), while, *GNB4* causes a dominant form of Charcot-Marie-Tooth (Soong et al., 2013).

**IDDCA/LADCI Syndromes**

In 2016 whole-exome sequencing successfully identified homozygous and compound heterozygous variants in the *GNB5* (NM_006578; MIM #617173) gene as the cause of IDDCA/LADCI (IDDCA, MIM #617173; LADCI MIM#617182) (Lodder et al., 2016; Shamseldin et al., 2016) syndromes. The transmission pattern of them was consistent with an autosomal recessive inheritance. Homozygous and compound heterozygous loss of function (LoF) pathogenic variants in *GNB5* gene were associated with a severe neurological phenotype including epileptic seizures, intellectual disability, delayed psychomotor development, hypotonia, and sick sinus syndrome (Figure 3).

**Figure 3**. IDDCA patient's phenotype

Additional finding includes visual abnormalities, with nystagmus and in some cases with reduction in cone and rode functions, and gastric reflux (Table 1) (Lodder et al., 2016). In contrast homozygous carriers of the most frequent missense variant p.(Ser81Leu) were characterized by the mildest form of the syndrome carrying mild intellectual disability in combination with language delay, attention-deficit/hyperactivity disorder, with or without cardiac arrhythmia (LADCI) (Shamseldin et al., 2016; Turkdogan et al., 2017; Malerba et al., 2018; Vernon et al., 2018). GNB5 mutations have been identified in various ethnic groups including Jordan, Puerto Rico, India, Morocco, Brazil, Saudi, Europe, Caucasus and Cambodia (Lodder et al., 2016; Shamseldin et al., 2016; Turkdogan et al., 2017; Malerba et al., 2018; Vernon et al., 2018). Since the first reports, additional affected individuals have been reported, delineating the spectrum of the phenotype with about 80% of them described with cardiac conduction dysfunction and 90% with severe intellectual disability. The disease prognosis is variable and in some instances lethal, particularly if the cardiac complications emerge as reported in (Turkdogan et al., 2017).

**Table 1**. Clinical features of IDDCA patients

| **Features** | **Prevalence %** |
|---|---|
| **Intellectual disability** | **90** |
| **Bradycardia** | **80** |
| Visual abnormalities | 65 |
| Seizures | 46 |
| Hypotonia | 73 |
| Verbal understanding | 50 |
| Speech development | 92 |
| Pathological gastric reflux | 26 |

References: (Lodder et al., 2016; Shamseldin et al., 2016; Turkdogan et al., 2017; Malerba et al., 2018; Vernon et al., 2018).

Consistent with manifestations present in affected human individuals we showed that treatment of *gnb5* zebrafish mutant knock out larvae with carbachol (CCh, a parasympathomimetic compound that activates acetylcholine receptors of the heart and the GNB5-RGS-GIRK channel pathway) resulted in a strong decrease of the heart rate, whereas it had little effect on wild-type and sibling larvae consistent with loss of negative regulation of the cardiac GIRK channel by GNB5-RGS. In contrast, treatment with the sympathetic agonist isoproterenol resulted in an increased heart rate that was similar in wild-type, sibling, and gnb5 mutant larvae (Lodder et al., 2016). These results indicate that *GNB5* is crucial for parasympathetic control of heart rate, but not for sympathetic control, suggesting that lack of *GNB5* is associated with extreme bradycardia at rest, highlighting the hypothesis that GIRK channels or any component of the signalling mechanism that regulates GIRK channel activity could be a potential therapeutic target for IDDCA.

**Gnb5 mouse models**

*Gnb5*-null mouse models have been described (Krispel et al., 2003; Zhang et al., 2011). Ablation of the mouse ortholog of *Gnb5* resulted in phenotypes reminiscent of those of IDDCA patient, specifically marked neurobehavioral abnormalities including learning deficiencies, hyperactivity, impaired gross motor coordination, abnormal gait (Zhang et al., 2011), defective visual adaptation (Krispel et al., 2003), perturbed development and

functioning of retinal bipolar cells (Rao et al., 2007), smaller body size in the pre-weaning period and high pre-weaning mortality. Moreover, whereas IDDCA patients show sinus bradycardia, which result in a dysfunction of the sinoatrial node in generating or transmitting an action potential to the atrial tissue, the cardiac phenotype of Gnb5 null animals has never been studied. Interestingly, mice lacking *Rgs6*, the *Gnb5*-dependent RGS protein that is enriched in heart tissue, or *Girk4* subunit, exhibited bradycardia and hypersensitivity to parasympathomimetics or diminished heart rate and heart rate variability responses to the cholinergic agonist (CCh), respectively (Posokhova et al., 2010; Kulkarni et al., 2018).

## AIM OF THE THESIS

Genomic approaches have led to the evidence that variants in *GNB1-5* genes cause a variety of human genetics diseases. However, the signalling responsible for these diseases is largely unknown, even though it likely involves dysfunction of ion channels. IDDCA/LADCI are a new autosomal recessive syndromes clinically well-defined, with no treatment or therapy available yet. The emerging involvement of *GNB5* mutations in patients with such diseases, strengthened our interest in the study of the disease. The phenotypic consequence of *GNB5* deficiency in affected individuals has its critical role in pathways specifically related to neuronal and cardiac functions. Specifically, since ~80% of affected patients showed cardiac arrhythmia, with ~20% of them were found death during sleep, probably due to sinus node dysfunction, we moved our interest to understand the effects of the cardiac phenotype shared in such patients driven by lack of functional *GNB5* at the functional level and to link it to clinical phenotype, thereby leading to an explanation for some of the pathogenic mechanisms of IDDCA.

Although immediate benefits for patients are unpredictable, this basic science study will hopefully unravel molecular pathways that will open the way to new therapeutic targets. We propose to dissect the pathogenic mechanisms at the molecular/functional level of a novel intellectual developmental disorder with cardiac arrhythmia (IDDCA, MIM#617173) by generating and characterizing human induced pluripotent stem cells (hiPSCs), hiPSC-derived cardiomyocyte (iCM) and hiPSC-derived neurons, of the pathology. Small-scale drug screening will be performed to identify compounds that may rescue the GNB5-associated phenotype.

# MATERIAL AND METHODS

**Self-replicate mRNA-based reprogramming of human induced pluripotent stem cell (hiPSC) lines**

Cell reprogramming, a derivation of human induced pluripotent stem cells (hiPSC) from somatic cells (Takahashi et al., 2007) provides an unlimited source for the possibility to model in culture dish any desired specialized cell, thus enabling the characterization of the biological mechanisms underlying the human pathology. We established hiPSC lines through a mRNA-based technology, an efficient method to generate integration free and virus-free human iPSCs using a single transfection step. It entails the use of a positive, single-stranded RNA species derived from non-infectious, self-replicating Venezuelan equine encephalitis (VEE) virus. This technology consists of a polycistronic, self-replicative RNA system that consistently express the reprogramming factors Oct4, Klf4, Sox2, and Glis1 (OKS-iG) (Figure 4) (Yoshioka et al., 2013).

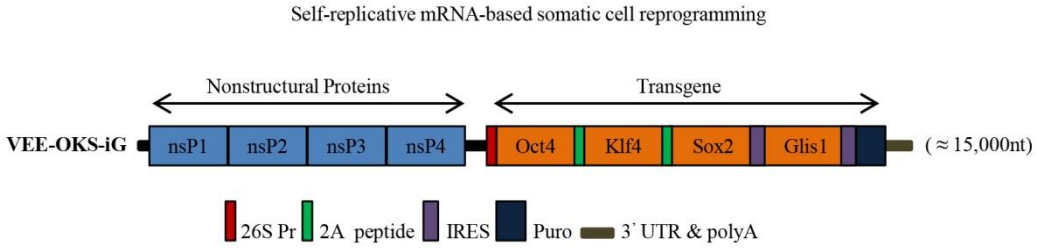


**Figure 4. Structure of the Simplicon™ RNA replicon.** The RNA replicon encodes four non-structural replication complex proteins (nsPs) as a single ORF in the 5'end of the RNA. At the 3'end, the viral structural proteins ORFs are replaced with the OKS-iG transgenes. Locations of 26S internal, 2A peptide, IRES and Puromycin (Puro)-resistance gene are indicated.

For reprogramming, $2x10^5$ fibroblasts were seeded on a 6-well plate (day 0) and maintained in fibroblast growth medium. The following day (day 1), the cells at 60-80% confluent were transfected using Simplicon™ RNA Reprogramming Kit (Merck-Millipore), according to manufacturer's instructions. During the next several days (day 2–4), 0.75µg/mL of puromycin was added in the Stage 1 Medium and was used to select for cells that have taken up the VEE-OKS-iG RNA. At day 10, RNA transfected cells puromycin-resistant at 70% confluent, were replated onto one 6-well plate containing inactivated mouse embryonic fibroblasts (MEFs) feeder cells, and cultured in Stage 2 Medium until colonies were manually isolated by picking. On day 28, individual hiPSC colonies were picked and re-seeded on 24-well plate

coated with Matrigel matrix (Corning) in feeder-free condition, cultured in Essential 8 Medium (Thermo Fisher Scientific) and propagated using ReLeSR (Stem Cell Technologies).

**hiPSC-derived cardiomiocytes differentiation**

Cardiomyogenic differentiation was performed by monolayer culture on hiPSC cultured in feeder free condition, plating 20,000 cells/$cm^2$ on 24-well plate coated with Matrigel, using PSC Cardiomyocyte Differentiation Kit (Thermo Fisher Scientific) that guarantees high yield of cardiac differentiation. After splitting, hiPSCs were allowed to grow to almost confluence and then maintenance medium were changed to medium A of the kit, which is designed to favour mesodermal differentiation. After 48h, medium was changed to medium B that induces differentiation of cardiac precursors and after other 48h the medium was changed to medium C that favours cardiomyocytes survival and maintenance. Around day 10 of differentiation, the culture starts to show spontaneous beating. Cells were kept in culture for allowing cell maturation and analysis were carried out at day 30. Spontaneously beating regions were manually dissected and plated on gelatin-coated dishes for further analyses.

**Karyotyping**

It is well known, that long-term culture induces genetic aberrations in pluripotent cell lines (Liang and Zhang, 2013). To assess the genome integrity of the genetic material, hiPSC were treated with 0.1 µg/mL colcemid (Gibco) for 1.5 h at 37°C in an atmosphere containing 5% $CO_2$. The cells were then treated with Accutase, washed in DPBS and incubate in a hypotonic solution (0,075M KCl pH7.0) for 25 min at 37°C. Thereafter the cells were fixed with methanol and glacial acetic acid (3:1 ratio) three times and stained with Giemsa stain (Gibco) on a glass slide (Fisher Scientific). The chromosomes were visualized with a 1000X objective (Zeiss, Germany) and analyzed by G-banding at GAG 300-400 band resolution in average, using Applied Imaging Cito-Vision (Version 7.5).

***GNB5* sequence mutation**

Genomic DNAs were extracted from fibroblasts and hiPSCs using Allprep DNA/RNA Mini kit (Qiagen Hilden, Germany), according to the manufacturer's instructions.

*GNB5* (MIM # 604447, NM_006578) mutations were confirmed by direct DNA sequencing for all patients and their available family members. PCR amplifications were carried out in a final volume of 50 µl consisting of:

- 50 ng genomic DNA
- 2.5 mM deoxyribonucleotides
- 15 pmol/µl of sense and antisense primers
- 1X Reaction Buffer (200mM Tris-HCl/ pH 8.8 at 25°), 100 mM KCl, 100mM (NH4)2SO4, 1.0% Triton X-100 and 21 mg/ml nuclease-free BSA) and
- 1 U of Taq DNA polymerase.

Denaturation was carried out at 95° for 30 s, annealing at 60°C for 30 s, extension at 72° for 30 s, for 35 cycles. Primers were designed using the Primer 3 Output program (http://frodo.wi.mit.edu/primer3/), amplicons and primers were checked both by BLAST and BLAT against the human genome to ensure specificity. The amplified products were subsequently purified (Exo Sap) and sequenced with a ready reaction kit (BigDyeTerminator v1.1 Cycle, Applied Biosystems). The fragments obtained were purified using DyeEx plates (Qiagen) and resolved on an automated sequencer (3130xl Genetyc analyzer DNA Analyzer, ABI Prism). Sequences were analyzed using the Sequencer software (Gene Codes, Ann Arbor, Michigan). All mutations were described following the recommendations of the Human Genome Variation Society (http://www.hgvs.org/mutnomen).

**Functional evaluation of *GNB5* variants**

Primary fibroblasts of family A affected individuals II.1 and II.2 (Lodder et al., 2016) were obtained from skin biopsies according to standard protocols. The cell cultures were maintained in DMEM/F12 supplemented with 10% FBS and 1% antibiotics mixture (penicillin and streptomycin 10.000 U/ml, Thermo Fisher Scientific) in a humidified atmosphere with 5% $CO_2$. Total RNA was obtained from primary fibroblasts using the RNeasy Mini kit (Qiagen) according to the manufacturer's specifications, and followed by DNase (Qiagen) treatment for the genomic DNA elimination. Retrotranscribed cDNA was synthesized from 1 µg of total DNA-purified RNA using the Quantitect Reverse Transcription Kit (Qiagen), according to the manufacturer's instructions. Synthesized cDNAs were used as templates for RT-PCR amplifications involving the region carrying the splice-site variant. To discriminate and tally expressed alleles cDNAs were amplified by PCR from the members of family A, inserted into the plasmid vector pCR™4-TOPO® (Life Technologies) and sequenced. Non-sense Mediated Decay (NMD) was assayed by treating fibroblasts with

Puromycin and Cycloheximide at a concentration of 200 µg/ml for 8h and 4h, respectively. After incubation, the fibroblasts were harvested, total RNA was extracted and RT-PCR reactions were performed. ImageJ software (U. S. National Institutes of Health, Bethesda, Maryland, USA) was used to quantify the intensity of the gel bands by first calibrating images using control bands and then manually selecting the bands for the measurement.

**Reverse Transcription (RT-PCR)**

1 µg RNA was reverse transcribed using the Quantitect Transcription kit (Qiagen). RT-PCR produces DNA copies (complementary DNA, or cDNA) of a RNA template, by using the enzyme reverse transcriptase, and the resulting single-stranded cDNA can be amplified using traditional or real-time PCR. Reverse transcriptase enzyme, in general, has 3 distinct enzymatic acitivities: an RNA-dependent DNA polymerase, a hybrid-dependent exoribonuclease (Rnase H), and a DNA-dependent DNA polymerase. For reverse transcription in vitro, the first 2 activities are utilized to produce single-stranded cDNA: RNA-dependent DNA-polymerase activity (reverse transcription) transcribes cDNA from an RNA template, and RNase H activity specifically degrades only the RNA in RNA: DNA hybrids. The purified RNA samples were incubated in 1X gDNA Wipeout Buffer at 42°C for 2 minutes to remove contaminating genomic DNA. After genomic DNA elimination, the RNA samples were reverse transcribed using a master mix prepared from Reverse Transcriptase (1U), 1X RT Buffer, and RT Primer Mix, a optimized blend of oligo-dT and random primers. The entire reaction was performed at 42°C for 30 minutes and then inactivated at 95°.

Each cDNA sample was measured by using a Nanodrop spectrophotometer (NanoDrop Technologies, Willmington, Delaware, USA) and used in qPCR for i) NMD-assay in primary fibroblasts, ii) evaluation of mRNA levels for *GNB5* expression, iii) hiPSCs characterization against pluripotency markers (OCT4, SOX2, NANOG, REX1 and LIN28), iv) iCMs characterization.

**Real-time polymerase chain reaction (qPCR)**

qPCR is a quantitative PCR method which enables both detection and quantification (as absolute number of copies or relative amount when normalized to DNA input or additional normalizing genes) of one or more specific sequences in a DNA sample.

Based on the molecule used for the detection, the real time PCR techniques can be categorically placed under two heads:

- non-specific fluorescent dyes that intercalate with double-stranded DNA, such as SYBR Green, which binds to the minor groove of the DNA double helix, and is the most widely used double-strand DNA-specific dye reported for real time PCR
- sequence-specific DNA probes consisting of oligonucleotides that are labeled with a fluorescent reporter, which permits detection only after hybridization of the probe with its complementary DNA target, such as Molecular Beacons, TaqMan Probes, FRET Hybridization Probes, Scorpion Primers.

Oligos for qPCR were designed using the Primer3 with default parameters. Amplicons and primer pairs were checked both by BLAST and BLAT against the human genome to ensure specificity.

Target genes expression was examined by amplification with the primer sets described in the Table 2.

**Table 2.** Oligos used for qPCR analysis

| Gene | Primer Forward | Primer Revers |
|---|---|---|
| **GNB5** | CCTTTGCTTCAGGGTCAGATG | TTTCTTTGGAATAGATGGCAACCT |
| **KLF4** | CTTCTTCACCCCTAGAGCTCATG | CGATCGTCTTCCCCTCTTTG |
| **LIN28** | CCGGACCTGGTGGAGTATTCT | CGCTTCTGCATGCTCTTTCC |
| **MYC** | TCTGGACCCATTCTGTTCAAAA | GCACATTAGACCCAGATGAACCA |
| **REX1** | CCTGCAGGCGGAAATAGAAC | GCACACATAGCCATCACATAAGG |
| **OCT4** | CGACCATCTGCCGCTTTG | GCCGCAGCTTACACATGTTCT |
| **KLF4** | GAAATTCGCCCGCTCAGA | CGGTGCCCCGTGTGTTTA |
| **SOX2** | CGCGATGCCGACAAGAA | AAAAATAGTCCCCCAAAAAGAAGTC |
| **TNNT** | AAGCCCAGGTCGTTCATGCCC | CTCCATGCGCTTCCGGTGGA |
| **HCN4** | GGTGTCCATCAACAACATGG | GCCTTGAAGAGCGCGTAG |
| **SHOX2** | GACGGAGGGTAGAAGGAAGC | CCTTTCGCATCCTCTTTGCG |
| **TBX18** | ATGGGTTTGGAAGCCTTGGT | ACTTGCATTGCCTTGCTTGG |
| **GAPDH** | GAAGGTGAAGGTCGGAGTC | GAAGATGGTGATGGGATTTC |

GAPDH was used as housekeeping genes. The reactions were run in triplicate in 10 µl of final volume with 10 ng of sample cDNA, 0.3 mM of each primer, and 1X Power SYBR Green PCR Master Mix (Applied Biosystems). Reactions were set up in a 384-well plate format with a Biomeck 2000 (Beckmann Coulter, Milan, Italy) and run in an ABI Prism7900HT (Applied

Biosystems) with default amplification conditions. Raw Ct values were obtained using SDS 2.3 (Applied Biosystems). Calculations were carried out by the comparative Ct method.

**Western Blotting analysis**

Protein extracts were resolved on home made 12% gels (for GNB5) and transferred to PVDF membranes (GE Healthcare) according to the manufacturer's instructions. Antibodies used were: mouse polyclonal antibody to anti-GNB5 (ptoteintech), and rabbit monoclonal anti-GNB5 (Abcam). Horseradish peroxidase conjugated anti-mouse (Santa Cruz), anti-rabbit (Santa Cruz) antibodies, and the ECL chemiluminescence system (GE Healthcare) was used for detection. Quantitation of band signal intensity was obtained by the ImageJ software (http://imagej.nih.gov/ij/). Values are expressed as fold differences relative to the wild-type protein sample, set at 1, after normalization for the loading control.

**Immunofluorescence staining**

The hiPSC cultures were fixed with 4% paraformaldehyde for 15 min at room temperature (RT). Fixed cells were washed twice in PBS, permeabilized and blocked for 30 min at RT with PBS containing 20% donkey serum and 0.1% TritonX-100. Cells were then incubated with primary antibodies for 2 h at RT in 20% donkey serum in PBS in oscillation, followed by three washing steps with PBS. The secondary antibodies were thereafter added for 1 h at RT in oscillation in the dark, followed by three washing with PBS, nuclei counterstain with DAPI (300mM) and image acquisition on Inverted Fluorescence Microscope (Axiovert 200M, Zeiss Carl; Software: AxioVision release 4.7.2 Dec 2008). Non-fixed hiPSC cultures were also incubated for StainAlive against TRA-1-60 antibody, to a final concentration of 2.5 µg/ml in fresh cell culture medium and incubate for 30 minutes at 37°C and 5% CO2. The cells were washed gently twice with cell culture medium and then were examined under an Inverted Fluorescence Microscope using the appropriate filters.

**GNB5 endogenous tagging via CRISPR/Cas9**

$2{,}5 \times 10^5$ hiPSC were plated in the matrigel-coated wells with 10µM of Rock inhibitor. After 24 hours, the cells were transiently transfected with GNB5_CRISPR/Cas9 KO Plasmid using the Lipofectamine 3000 reagent according to manufacturer's instructions. The GNB5_CRISPR/Cas9 KO Plasmid system consists of a pool of 3 plasmids (Table 3), each

encoding the Cas9 nuclease and a different target-specific 20 nt guide RNA (gRNA) designed for maximum knockout efficiency.

**Table 3.** Gβ5 CRISPR/Cas9 KO Plasmid (h) gRNA plasmids

| | |
|---|---|
| **gRNA A** | Sense: GCCAAATACATTAACGAGAA |
| **gRNA B** | Sense: ACCTTTCTCGTTAATGTATT |
| **gRNA C** | Sense: CTTTGCACCAGTCCATGCAC |

After 48 hours, we enriched the transfected cells by FACS analysis based on their EGFP fluorescent signal. The pool of FACS-isolated transfected hiPSCs were plated into matrigel-coated 10cm plate and cultivated sparsely. After approximately 20 days colonies were large enough for their manual picking and expansion. Each clone isolated were analyzed for genome modifications by Sanger Sequencing.

**Electrophysiological analysis**

The recording of action potentials was performed on small aggregates of dissociated cardiomyocytes between day 28 and day 33. Patch-Clamp experiments were conducted between 48 and 72 hours after isolation (between day 30 and 35) in Whole-Cell configuration and in Current Clamp mode.

During the experiment, the cardiomyocytes are kept at a constant temperature of 37 ° C and continuously perfused with a physiological solution (Tyrode) as follows: NaCl 137 mM, KCl 5 mM, CaCl2 2 mM, MgCl2 1 mM, HEPES-NaOH 10 mM , D-Glucose 10 mM, pH = 7.4. The borosilicate micropipettes had a resistance of 7-8MΩ used once filled with an intracellular solution thus composed: K-aspartate 130 mM, 10 mM NaCl, 5 mM EGTA-KOH, 10 mM Hepes, 2 mM CaCl2, 2 mM MgCl2, ATP (Na + -sel) 2 mM, Creatine Phosphate 5 mM, GTP (Na + -salt) 0.1 mM, pH = 7.2.

To evaluate the response to modulators of the frequency of action potentials, the cardiomyocytes were perfused with Tyrode added with 100 nM charbacol, (CCh) a stable agonist of $M_2$-muscarinic receptors or with Tertiapin-Q, a blocker of the GIRK channels and compared with the frequency in only tyrode to evaluate the increase or the decrease. For the analysis of electrophysiological data, the Clampfit 10.6 and OriginPro 2016 software was used.

**Transcriptome profiling by RNA-Seq**

For transcriptome profiling we performed RNA-seq using paired-end sequences of poly-A RNA after rRNA removal and fragmentation steps. Libraries were prepared using Illumina TruSeq RNA Library Prep Kit v2. Paired-end 75 bp sequence reads were generated with the Illumina NextSeq500 platform, reaching high coverage (~40M reads per sample). We processed three biological replicates for each cell line, a number that will assure the removal of intra-sample variability and potential outliers.

We used the RAP pipeline (D'Antonio et al., 2015)– part of the CINECA's bioinformatics resources – to process and analyse the RNA-seq data.

# RESULTS

## Recruitment of IDDCA patients

Since 2016, when the syndrome was identified, 26 patients with 12 different *GNB5* variants (Figure 5) have been identified (Lodder et al., 2016; Shamseldin et al., 2016; Turkdogan et al., 2017; Malerba et al., 2018; Vernon et al., 2018) (Merla and Malerba, unpublished). The clinical evaluation included medical history interviews, a physical examination and review of medical records (Table 4). The following types of *GNB5* mutations have been identified: 6 frameshift (6/12, 50%), 3 missense (3/12, 25%), and 3 nonsense (3/12 25%). All the *GNB5* identified variants were inherited from asymptomatic parents.

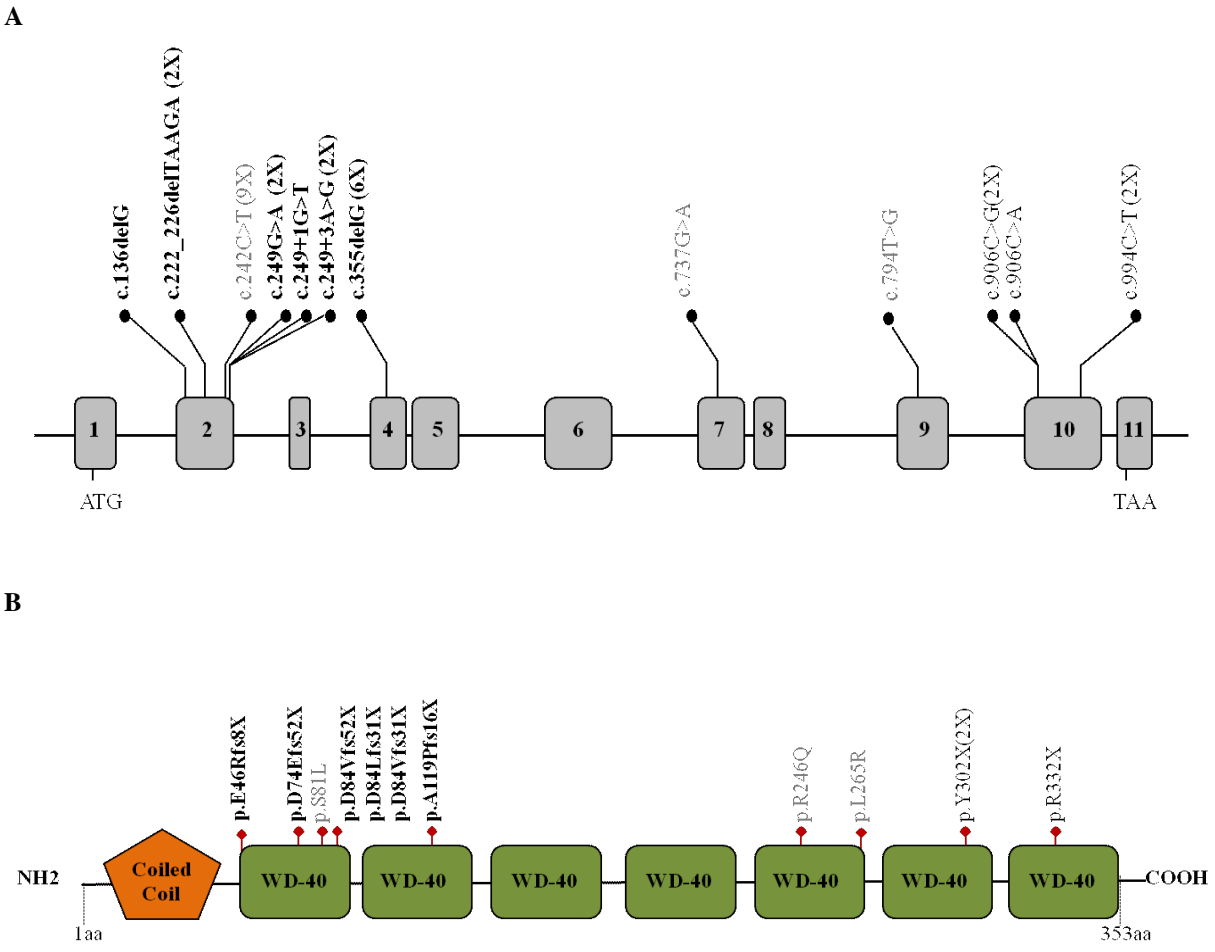


**Figure 5.** (A) Distribution of the GNB5 variants (NM_006578) across the gene with exons indicated by grey boxes. The frameshift variants are designated in bold, missense variants are in gray, and nonsense variants are in black. The number of patients with each variant is indicated in parentheses. (B) Schematic representation of the GNB5 protein with Coiled coil and WD-40 repeats domains.

**Table 4.** Clinical features of GNB5-patients reported so far

| | Lodder et al., 2016 Family A II.1 | Lodder et al., 2016 Family A II.2 | Lodder et al., 2016 Family B | Lodder et al., 2016 Family C II.2 | Lodder et al., 2016 Family C II.3 | Lodder et al., 2016 Family D | Lodder et al., 2016 Family E II.1 |
|---|---|---|---|---|---|---|---|
| **Paternal allele** | c.249G>A p.Asp84Valfs*52 | c.249G>A p.Asp84Valfs*52 | c.249+1G>T p.Asp84Leufs*31 | c.249+3A>G p.Asp84Valfs*31 | c.249+3A>G p.Asp84Valfs*31 | c.906C>G; p.Tyr302* | c.242C>T; p.Ser81Leu |
| **Maternal allele** | c.994C>T p.Arg332* | c.994C>T p.Arg332* | c.249+1G>T p.Asp84Leufs*31 | c.249+3A>G p.Asp84Valfs*31 | c.249+3A>G p.Asp84Valfs*31 | c.906C>G; p.Tyr302* | c.242C>T; p.Ser81Leu |
| **Gender, age (years)** | F, 24 | F, 22 | F, 8 | F, 13 | M, 11 | F, 14 | F, 15 |
| **Birth weight (percentile)** | 3,580 g (50th) | NA | 2,980 g (15th) | 2,751 g (15th) | NA | 2,845 g (15th) | NA |
| **Ethnicity** | Italy | Italy | Jordan | Puerto Rico | Puerto Rico | India | Morocco |
| **Consanguinity** | – | – | + | + | + | – | – |
| **Verbal understanding** | NA | NA | nonverbal | unremarkable | unremarkable | NA | NA |
| **Speech Development** | + | + | nonverbal | nonverbal | delayed | nonverbal | + |
| **Intellectual disability** | Severe ID | Severe ID | Severe ID | Severe ID | Global developmental delay | Severe ID | Mild ID |
| **Epilepsy** | + | + | + | – | – | + | – |
| **Retinal Disease** | NA | Retinal degeneration | NA | NA | NA | + | NA |
| **Nystagmus** | + | + | + | + | + | + | NA |
| **Sinus sick syndrome** | + | Bradyarrhythmia | + | + | + | increased PR interval (intermittent Wenckebach) | + |
| **Minimum heart rate (bpm)** | 24 | 39 | NA | paced | paced | NA | 20 |
| **Maximum heart rate (bpm)** | 163 | 192 | NA | paced (27% heartbeats on Holter) | paced (20% heartbeats on Holter) | NA | 176 |
| **Chronotropic response** | NA | NA | NA | + | + | NA | unremarkable |
| **Escape beats** | + | + | NA | paced | paced | NA | + |
| **Pacemaker implantation** | – | – | – | + | + | – | – |
| **Cardiac anomalies** | – | PFO | NA | – | – | – | – |
| **Hypotonia** | + | + | + | + | + | + | – |
| **Gastroesophageal Reflux** | + | + | – | + | + | + | – |
| **Others** | | | | Abnormally mithocondrial shape, focal z-band streaming and type1 fiber predominance | | | |

| | Lodder et al., 2016 Family E II.3 | Lodder et al., 2016 Family F | Shamseldin et al., 2016 V:1 | Shamseldin et al., 2016 V:2 | Shamseldin et al., 2016 V:3 | Shamseldin et al., 2016 IV:1 | Shamseldin et al., 2016 IV:6 |
|---|---|---|---|---|---|---|---|
| **Paternal allele** | c.242C>T; p.Ser81Leu | c.242C>T, p.Ser81Leu | c.242C>T, p.Ser81Leu | c.242C>T, p.Ser81Leu | c.242C>T, p.Ser81Leu | c.242C>T, p.Ser81Leu | c.242C>T, p.Ser81Leu |
| **Maternal allele** | c.242C>T; p.Ser81Leu | c.242C>T, p.Ser81Leu | c.242C>T, p.Ser81Leu | c.242C>T, p.Ser81Leu | c.242C>T, p.Ser81Leu | c.242C>T, p.Ser81Leu | c.242C>T, p.Ser81Leu |
| **Gender, age (years)** | M, 10 | M, 25 | F, 12 | F, 11 | F, 5 | F, 7 | F, 11 |
| **Birth weight (percentile)** | NA | NA | 50th centile | 50th centile | NA | 50th centile | NA |
| **Ethnicity** | Morocco | Brazil | Saudi | Saudi | Saudi | Saudi | Saudi |
| **Consanguinity** | – | + | + | + | + | - | - |
| **Verbal under standing** | NA | NA | + | + | + | + | + |
| **Speech Development** | + | NA | Severe language delay | Severe language delay | Severe language delay | Severe language delay | Severe language delay |
| **Intellectual disability** | Mild ID | Mild ID | normal IQ, but school performance issues | normal cognitive development | NA | normal IQ | NA |
| **Epilepsy** | – | – | NA | NA | NA | NA | NA |
| **Retinal Disease** | NA | NA | NA | NA | NA | NA | NA |
| **Nystagmus** | – | NA | NA | NA | NA | NA | NA |
| **Sinus sick syndrome** | + | + | NA | NA | NA | NA | NA |
| | | | NA | NA | NA | NA | NA |
| **Minimum heart rate (bpm)** | 16 | | NA | NA | NA | NA | NA |
| **Maximum heart rate (bpm)** | 180 | NA | NA | NA | NA | NA | NA |
| **Chronotropic response** | unremarkable | NA | NA | NA | NA | NA | NA |
| **Escape beats** | + | NA | NA | NA | NA | NA | NA |
| **Pacemaker implantation** | + | NA | NA | NA | NA | NA | NA |
| **Cardiac anomalies** | – | NA | NA | NA | NA | NA | NA |
| **Hypotonia** | impaired fine motor skills | – | - | - | NA | + | NA |
| **Gastroesophageal Reflux** | – | NA | | | | NA | NA |
| **Others** | | | ADHD, Hyperactivity | Inattentive type ADHD | motor delay | motor delay | ADHD, mild motor delay |

| | Turkdogan et al., 2017 V.1 | Turkdogan et al., 2017 IV.14 | Vernon et al., 2018 | Malerba et al., 2018 | Poke and Sadleir 2017 (unpublished) | Poke and Sadleir 2017 (unpublished) | Kannu and Shao 2018 (unpublished) | Kannu and Shao 2018 (unpublished) |
|---|---|---|---|---|---|---|---|---|
| **Paternal allele** | c.355delG; p.Ala119Profs*16 | c.355delG; p.Ala119Profs*16 | c.737G>A; p.Arg246Gln | c.222_226delTAAGA; p.Asp74Glufs*52 | c.906C>G; p.Tyr302* | c.136delG; p.Glu46Argfs*8 | c.794T>G; p.Leu265Arg | c.906C>A; pTyr302* |
| **Maternal allele** | c.355delG; p.Ala119Profs*16 | c.355delG; p.Ala119Profs*16 | c.222_226delTAAGA; p.Asp74Glufs*52 | c.242C>T; p.Ser81Leu | c.906C>G; p.Tyr302* | c.136delG; p.Glu46Argfs*8 | c.794T>G; p.Leu265Arg | c.906C>A; pTyr302* |
| **Gender, age (years)** | M, 3 | F,11 | M, 2 | F, 2.5 | M,2.5 | M, 10 | F, 9 | F, 3 |
| **Birth weight (percentile)** | NA | 1800 g (<1st) | 3311 g (50th) | 1698 g (<1st) (Intrauterine growth restricted) | 3300g (50th) | 2740g (3rd) | 2585 g (25-50%tile) | No records but 7.49kg at 5 months |
| **Ethnicity** | NA | NA | European/Caucasian | European/Caucasian | Pakistan | Cambodian | Cambodian | South Asian |
| **Consanguinity** | + | + | – | – | First cousins once removed | Second cousins | + (Maternal grandmother is Paternal grandmother sister) | - |
| **Verbal understanding** | "no developmental milestones" | "no developmental milestones" | nonverbal | + | noverbal | nonverbal | limited | - |
| **Speech Development** | "no developmental milestones" | "no developmental milestones" | nonverbal | expressive speech delay | nonverbal | nonverbal | fourteen months | Severe language delay |
| **Intellectual disability** | Severe ID | Severe ID | Severe ID | Mild ID | Severe DD | Severe ID | severe ID | Severe ID |
| **Epilepsy** | + | + | – | – | + | + | - | EEG showed slow wave, no seizure |
| **Retinal Disease** | Retinal degeneration | Retinal degeneration | Severe reduction in cone and rode function | – | NA | No (normal examination 2010) | Bilateral high myopia | Cortical blindness, ERG anmoral wave forms |
| **Nystagmus** | + | + | + | strabismus | roving eye movements, vertical nystagmus | roving eye movements | - | + |
| **Sinus sick syndrome** | Sinus arrhythmia/ Sinus bradycardia | Sinus arrhythmia/ Sinus bradycardia | Sinus arrhythmia/ Sinus bradycardia | + | + | + | Sinus bradycardia | + Sinus bradycardia with skips |
| **Minimum heart rate (bpm)** | NA | NA | 71 | 36 | NA | NA | 38 | 28 |
| **Maximum heart rate (bpm)** | NA | NA | 183 | 176 | NA | NA | 171 | 151 |
| **Chronotropic response** | NA | NA | NA | NA | + | | NA | NA |
| **Escape beats** | NA | NA | + (prior to pacing) | + | + | + | - | + |
| **Pacemaker implantation** | Refused by parents | Refused by parents | + | + | - | - | - | - |
| **Cardiac anomalies** | – | – | – | – | - | - | - | - |
| **Hypotonia** | + | + | + | + | + | + | - | +++ |
| **Gastroesophageal Reflux** | normal (abdominal US examination) | normal (abdominal US examination) | + | – | - | + | - | - |
| **Others** | autistic (midline hand automatism, no eye contact) | autistic (midline hand automatism, no eye contact) | hypertonia Laryngomalacia hypertonia, | ear tubes | | | No dystonia. Non dysmorphic | Motor delay |

**GNB5 nonsense and frameshift variants**

The prevalence of *GNB5* variants found in our cohort is predicted to lead to truncated protein suggesting a loss of function event. In order to investigate the possibility that GNB5 mRNA carrying truncating variants may result in the partial transcripts degradation, we investigated the nonsense-mediated mRNA decay pathway. The r.[249G>A; 249-250ins25] allele is predicted to encode a truncated polypeptide containing a stretch of 52 incorrect amino acids starting with an Asp to Val substitution at position 84 (p.(Asp84Valfs52X)). Cloning and sequencing of amplicons from individual A.II.1 and A.II.2 (Lodder et al., 2016) further revealed that all transcripts containing the paternal allele were aberrantly spliced. Using the same approach, we examined the relative abundance of the c.249G>A and c.994C>T alleles. Both altered transcripts are less frequent than their unchanged counterpart in parents' cells of (A.I.2) and father (A.I.1) (5 out of 14 amplicons (35.7%) for the paternal allele and 2 out of 15 (13.3%) for the maternal one). These results prompted us to hypothesize that both mutant alleles of family A might be targeted by nonsense-mediated mRNA-decay (NMD) pathway. We measured by RT-PCR the levels of *GNB5* mRNA in proband's fibroblasts after treatment with puromycin or cycloheximide, two known NMD inhibitors. The mRNA level of *GNB5* was restored after treatment with both NMD inhibitors suggesting that the c.249G>A and c.994C>T variants trigger NMD of the corresponding transcripts and thus represent LoF alleles (Figure 6).

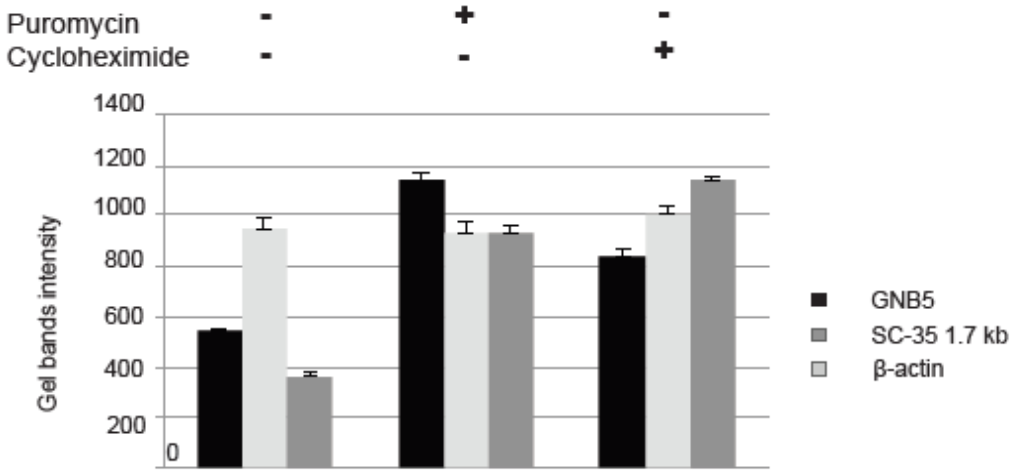


**Figure 6. Molecular characterization of Family A variants.** The physiological NMD substrate SC-35 1.7 Kb was included as positive control (dark grey bars). β-actin (light grey bars) was used as internal control.

**Generation of hiPSCs from patients and controls skin fibroblasts**

Starting from skin biopsy, we generated primary fibroblast cell lines from all members of the Family A described in (Lodder et al., 2016), that consists of two severely affected sibling carrying compound heterozygous p.Asp84Valfs52*/Arg332* (p.D84Vfs52X/p.R332X) *GNB5* variants and their heterozygous healthy carrier parents, as well as an additional patient carrying compound heterozygous p.Asp74Glufs52*/Ser81Leu (p.D74Efs8X/p.S81L) *GNB5* variants (Malerba et al., 2018). Thanks to already settled collaborations we got skin fibroblasts from three novel unpublished cases bearing the homozygous frameshift variants p.Glu46Argfs8*, the nonsense mutation p.Tyr302*, and the missense homozygous variant p.Leu265Arg respectively (Figure 7).

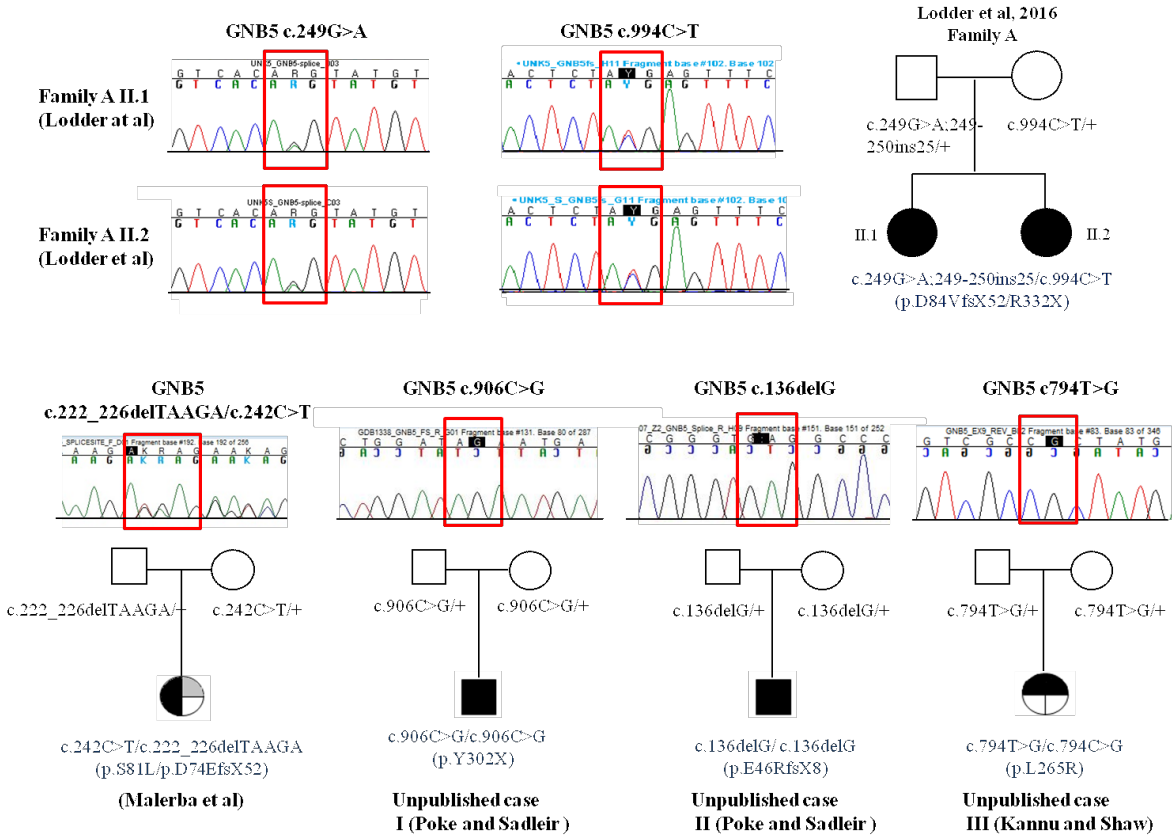


**Figure 7**. Sanger Sequence electropherogram of the GNB5 mutations in fibroblast cohort of IDDCA patients

Skin fibroblast derived-hiPSC lines have been established according to standard protocol (Figure 8) (See Material and Methods), and characterized from all the individuals reported in Table 5, along with those from two heterozygous healthy carrier parents and four unrelated healthy controls.

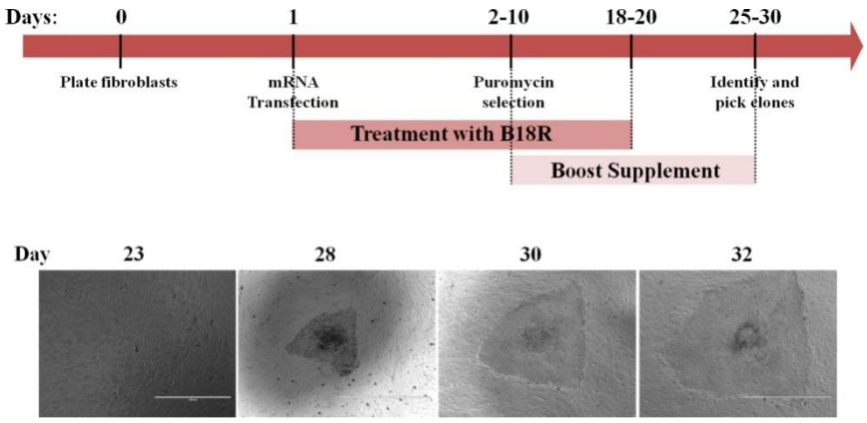


**Figure 8. Generation of IDDCA patients-derived hiPSC lines by integration-free, virus-free reprogramming.** (Above) Key steps and media requirements are indicated: i) plating of skin fibroblasts in fibroblast medium; ii) administration of synthetic mRNAs alongside the B18R inhibitor of interferon response; and iii) identification and picking of suitable hiPSC clones. (Below): Representative time course of human hiPS colonies generated using Human Simplicon RNA Reprogramming Kit. Colonies start to emerge from Day 25-28 and are ready to be picked at Day 32.

**Table 5.** Genotype of IDDCA patient-derived hiPSC lines. Of note, hiPSC from six healthy (GNB5 wild-type genotype) individuals have been also generated as control cohort. Gender and age is reported for each hiPSC cell line. F, female. M, male. GDB, Biobank identification code.

| | **Lodder et al., 2016 Family A II.1** **GDB 813** | **Lodder et al., 2016 Family A II.2** **GDB 813-6** | **Malerba et al., 2018** **GDB 1337** | **Unpublished case II (Poke and Saldeir)** **GDB 1307_Z2** | **Unpublished case III (Kannu and Shao)** **GDB 1378** |
|---|---|---|---|---|---|
| **Paternal allele** | c.249G>A p.D84Vfs52X | c.249G>A p.D84Vfs52X | c.222_226delTAAGA p.D74Efs52X | c.136delG p.E46Rfs8X | c.794T>C p.L265R |
| **Maternal allele** | c.994C>T p.R332X | c.994C>T, p.R332X | c.242C>T, p.S81L | c.136delG, p.E46Rfs8X | c.794T>C p.L265R |
| **Gender, age (ys)** | F, 24 | F, 22 | F, 3 | M 10 | F, 9 |

Cells that showed morphological evidence of reprogramming were selected manually. Two independent hiPSC clones per individual have been characterized (Figure 9-10) using standard methods by i) growth kinetics and maintenance of undifferentiated morphology upon culturing in feeder-free conditions; ii) expression of standard human pluripotency markers by immunofluorescence (against OCT4, NANOG, SOX2, and TRA-1-60); iii) quantitative RT-PCR evaluation of pluripotency markers (NANOG, OCT4, LIN28, and SOX2); and iv) Short Tandem Repeat (STR) and karyotyping analysis to confirm clones identity and genomic integrity, respectively. Mutation of GNB5 was confirmed by Sanger Sequencing.

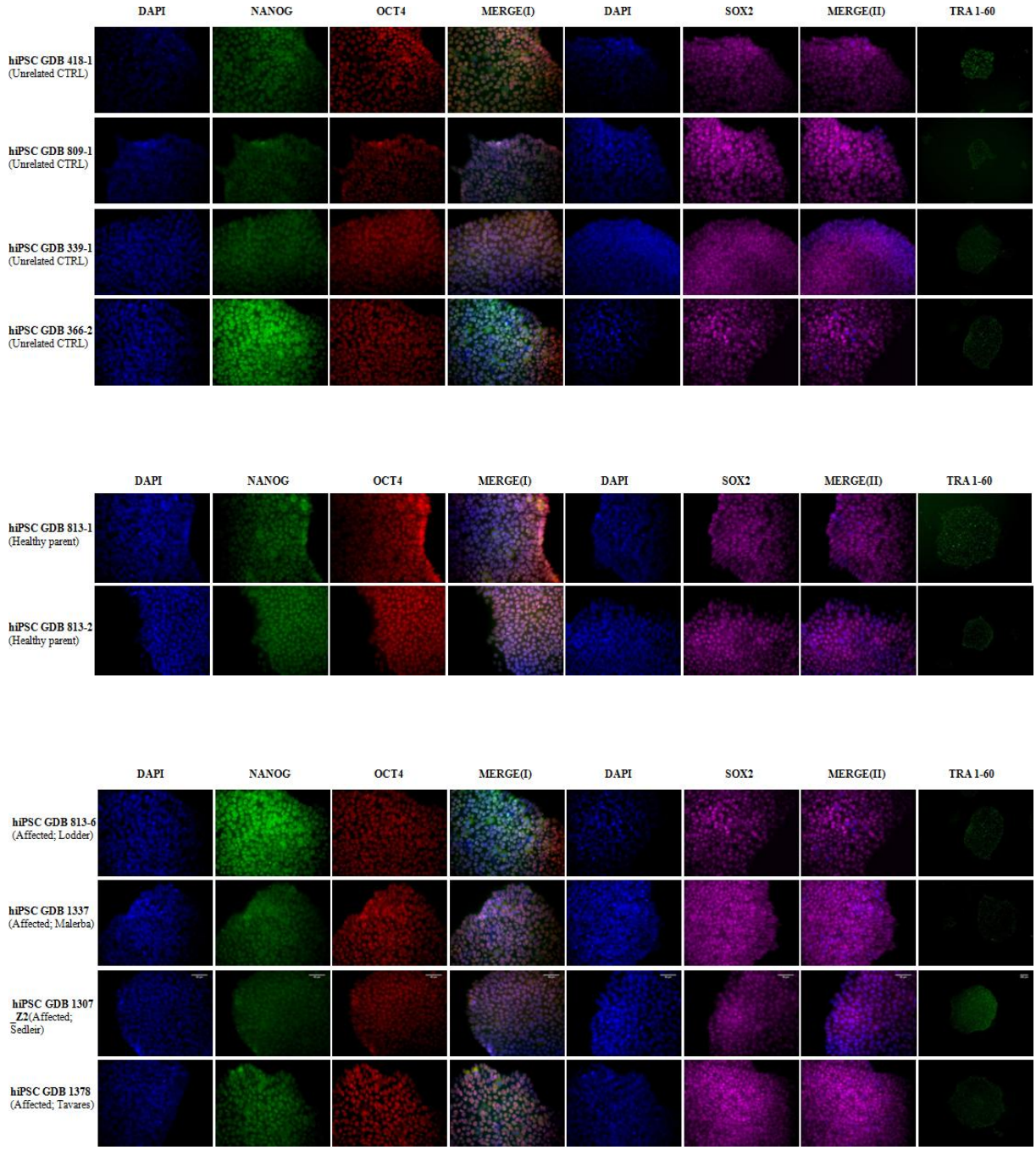


**Figure 9.** Representative characterization of unrelated controls, healthy parents and IDDCA patients-derived hiPSC lines by Immunofluorescence detection for expressing pluripotency markers NANOG, OCT4 SOX2, and TRA-1-60. Nuclei were stained with DAPI (blue). Images acquired with fluorescence microscope 40X magnification.

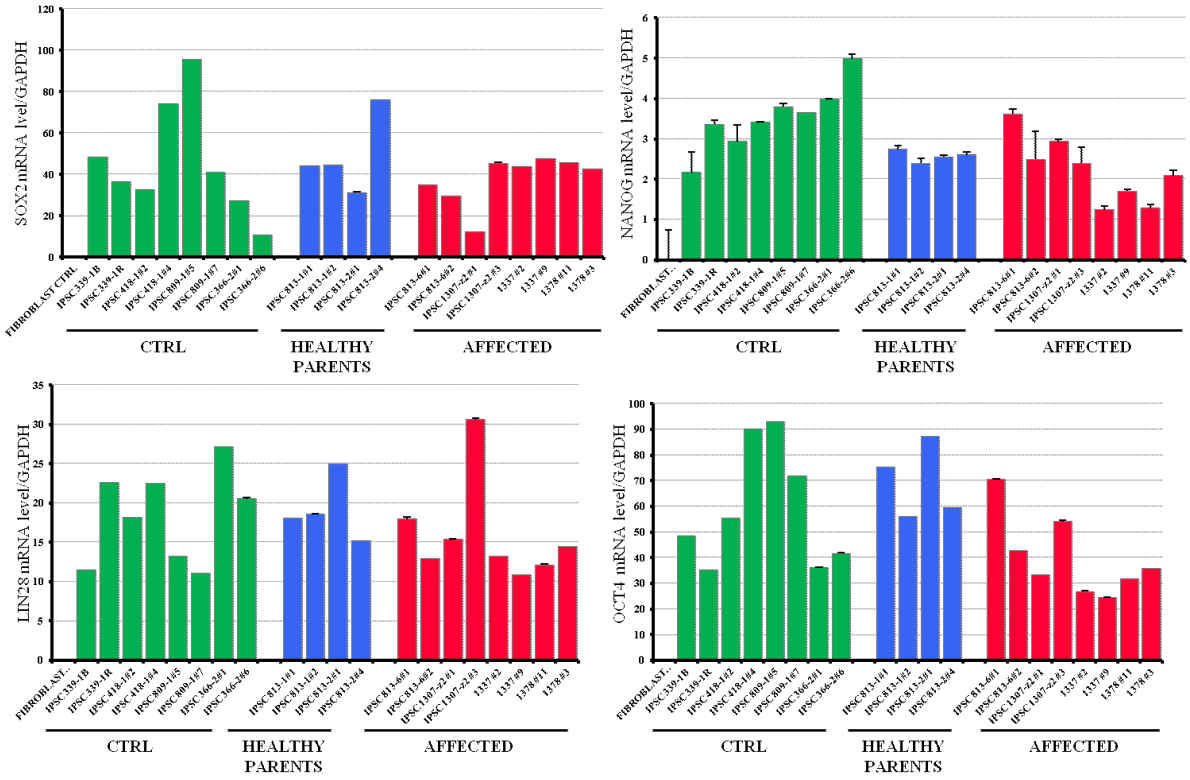


**Figure 10.** Quantification of pluripotency markers by RT-qPCR. The expression of endogenous pluripotency-associated markers SOX2; NANOG; LIN28, and OCT4 were confirmed by RT-qPCR in all fibroblast-derived hiPSC lines. A primary fibroblast (FIBROBLAST CTRL) was used as negative control. The results of three independent experiments are expressed as mean ± SD.

## Analysis of the GNB5 gene expression

GNB5 mRNA levels were measured by RT-qPCR in primary skin fibroblasts, 5 from IDDCA patients, 2 from healthy parents and 2 unrelated controls. We performed three RT-qPCR experiments (each in triplicate) to quantify the relative transcript concentrations of the corresponding gene, by using the comparative cycle threshold (Ct) method with the formula: 2^(ΔCt). Each input was normalized to *GAPDH*.

As reported in Figure 11 (upper panel), the endogenous *GNB5* mRNA expression level was consistently decreased in healthy parents (blue) and in affected patients (pink) when compared to unrelated controls (green), suggesting the correlation between the genotype and the gene dosage.

This data was also confirmed in our cohort of fibroblasts and fibroblast-derived hiPSCs by RNA-Seq analysis as shown in Figure 11 (low panel).

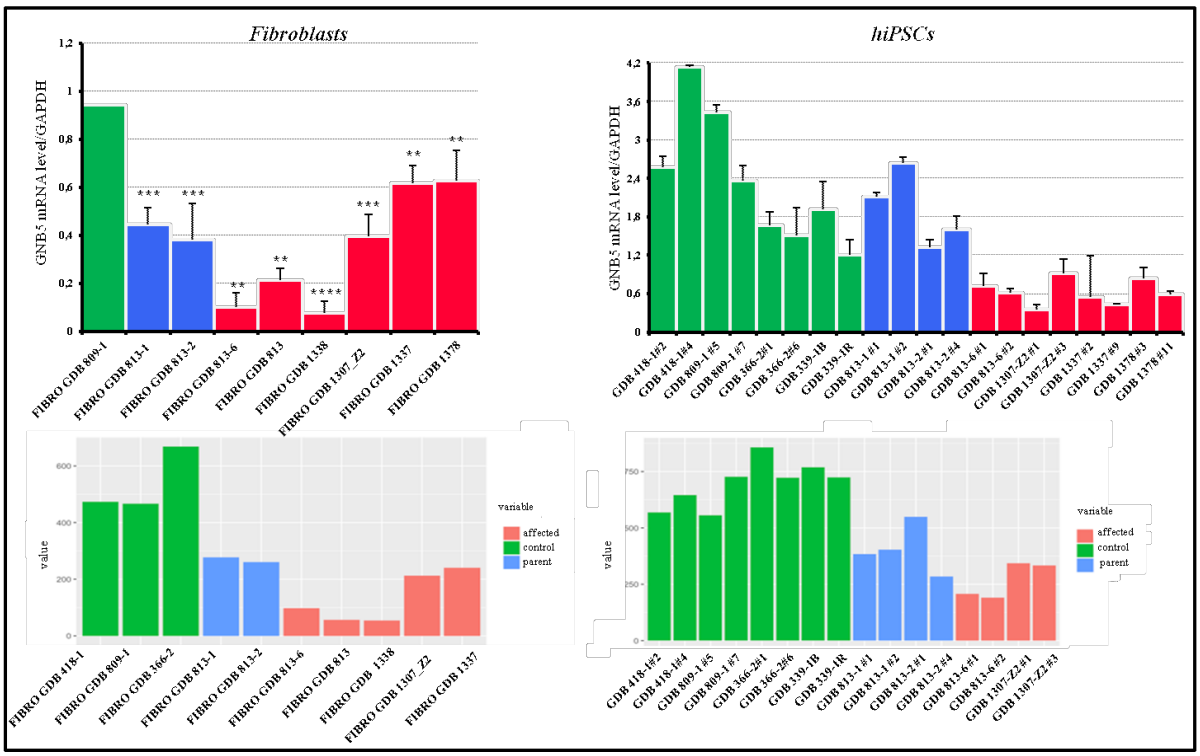


**Figure 11.** GNB5expression levels on primary skin fibroblasts and hiPSCs included in our study. Upper panel; data from RT-qPCR analysis. Low panel; data from RNA-Seq assay. The results of three independent experiments are expressed as mean ± SD. Student's t-test (*: p-value <0.01; **: p-value <0.001; ***: p-value <0.0001; ****: p-value <0.0001).

## Generation and selection of GNB5 hiPSC_KO

The skin fibroblast-derived hiPSC lines selected in this study (4 from IDDCA patients, 2 from healthy parents and 4 from unrelated controls) represent our cohort of patient-specific. In order to gain deeper insight into GNB5 function in IDDCA patients, we selectively knocked-down (KO) its expression via CRISPR-Cas9 system. hiPSC_GNB5_KO (hiPSCKO) and hiPSC_WT (hiPSCWT) isogenic cell lines have been preferred to patient and control-derived hiPSC lines to keep the same genotypes through the whole study and to avoid the genotype-intrinsic influence of each IDDCA patient and control cell lines.

The PCR amplification and Sanger Sequencing have been performed on extracted DNA of the same hiPSCs, showed a deletion of five nucleotides (c.204_208delCATGG) in exon 2 of the gene, which gives rise a premature stop codon of the protein, p.C68fsX, confirmed by Sanger sequencing on RT-PCR amplicon (Figure 12A). We confirmed that the cell lines showed a normal karyotype (Figure 12B). Moreover, the absence of the GNB5 protein and the decrease of its expression level in hiPSCKO cells were evaluated by Western blot and RT-qPCR, respectively (Figure 12C-D).

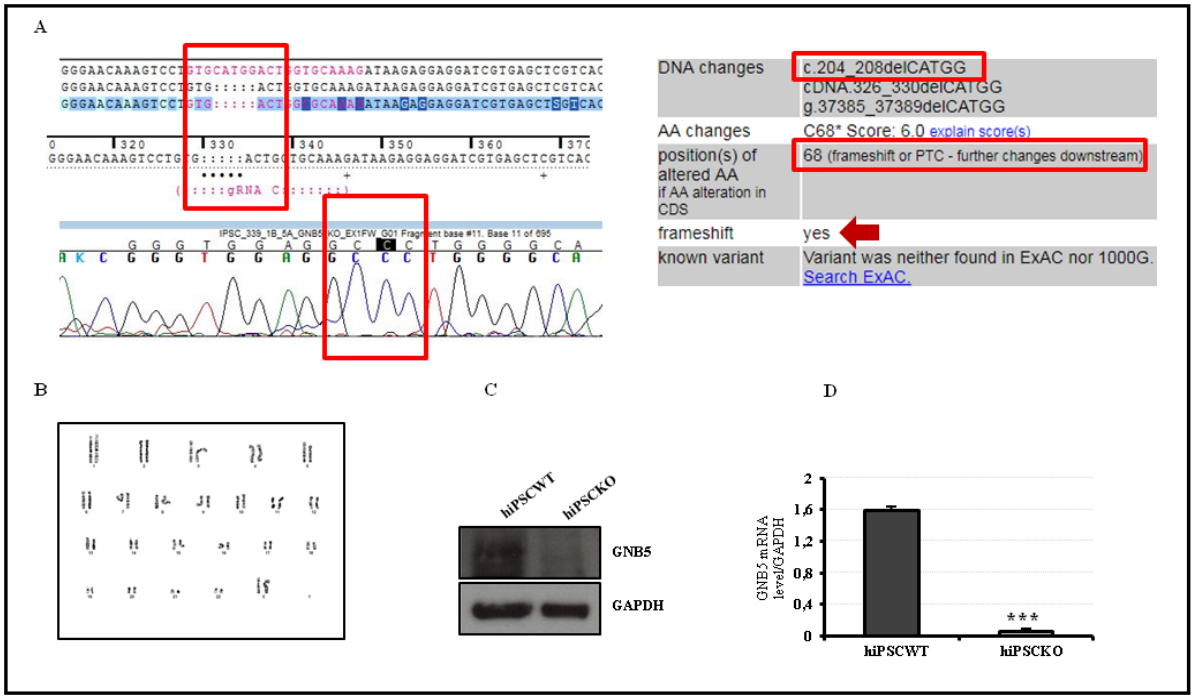


**Figure 12. Characterization of hiPSCKO cell line.** (A) Sanger sequencing on RT-PCR amplicon; (B) hiPSC KO karyotype analysis, (C) absence of the GNB5 protein in hiPSCKO by Western blot and (D) decrease of its mRNA expression levels by RT-qPCR. Student's t-test (*:p-value< 0.01; **p-value< 0.001; ***p-value< 0.0001).

We generated three independent clones each for KO, each carrying the same mutation c.204_208delCATGG. The presence of off-targets, predicted by target sites prediction tool (https://crispr.cos.uni-heidelberg.de/) was ruled out by PCR and Sanger Sequencing analysis of the *in silico* predicted off targets genes.

**Table 6.** Oligos used for off targets genes analysis

| Gene | Primer Forward | Primer Revers |
|---|---|---|
| **IGSF6** | TGGACTACACTCATGAGGCC | GTATGAAGGCCACGCACAC |
| **MAST2** | TGAGGCCTCCCATCATCATC | GGGAGCTGCTCTGTGATGAA |

### Generation and characterization of hiPSC-derived cardiomyocytes (iCM)

The use of animal models have greatly contributed to our understanding of the etiology and mechanisms of diseases; however due to interspecies physiologic differences between human and animal cardiomyocytes in terms of cell biological, mechanical and electrophysiological properties animal model do not accurately represent the physiology of human cardyomyocites (CMs) (Denayer et al., 2014).

Thanks to hiPSCs thechnology now it is possible to study human cardiac physiology and cardiac disease development in culture by providing an unlimited access to all cell types of the heart. The heart is the muscular organ made up of a variety of cells, in which cardiomyocytes (CMs) make up about one-third of all of the cells in the heart and are the fundamental work unit responsible for conduction of electrical impulses and contraction of cardiac muscle (Devalla et al., 2015). hiPSC-derived cardiomyocytes are similar to human cells both structurally and electrophysiologically and contract at a rate similar to human heart (Coskun and Lombardo, 2016).

Cardiac differentiation (2 independent clones for each hiPSC line), was assessed following to manufacturer's instructions (Figure 13) (See Material and Methods).

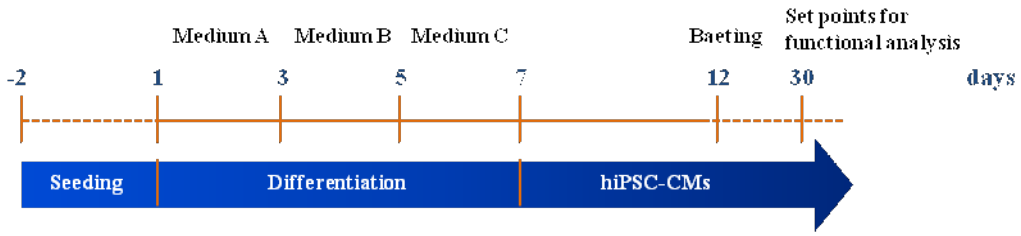


**Figure 13.** Schematic representation of hiPSCs-derived cariyomyocites (iCM) differentiation protocol

Initially, the hiPSCKO and hiPSCWT isogenic cell lines have been preferred to patient and control-derived hiPSC lines to keep the same genotypes through the whole study and to avoid the genotype-intrinsic influence of each IDDCA patient and control cell lines, thereby confounding the evaluation of screening and phenotyping assays.

Since a hallmark of IDDCA is sinus node dysfunction, we increased the yield of pacemaker-like cells by incubating differentiating iCM with 1mM 1-ethyl-2-benzimidazolinon (Jara-Avaca et al., 2017). At day 30 of differentiation, necessary to obtain cells with a good degree of maturation in term of electrical activity, spontaneously beating regions were enzymatically and mechanically isolated and cardiomyocytes were seeded on fibronectin-coated dishes for further analyses. Figure 14A shows representative confocal images of isolated iCM stained with antibodies against the cardiac TnT (red), organized in sarcomere-like structures, and with an antibody anti-GNB5 showing that the protein is expressed in the WT line (**iCMWT**) but not in the GNB5 KO line (**iCMKO**). The lack of GNB5 protein expression in iCMKO was confirmed by Western Blot analysis (Figure 14B).

To evaluate the efficiency of iCM differentiation protocol, at day 30-35 of maturation, expression analysis of cardiac troponin T (*TNNT*; TnT) was evaluated by RT-qPCR as reported in Figure 14C. Specifically, the expression level of TNNT was equally expressed between the two populations (iCMWT and iCMKO), to mean that the efficiency of differentiation was comparable across all the lines.

Moreover, the expression analysis of the markers typical of the sinus node commitment (*TBX18* and *SHOX2*) and function (*HCN4*) (Barbuti and Robinson, 2015), were significantly less expressed in iCMKO, a result compatible with the sinus node dysfunction typical of IDDCA (Figure 14C).

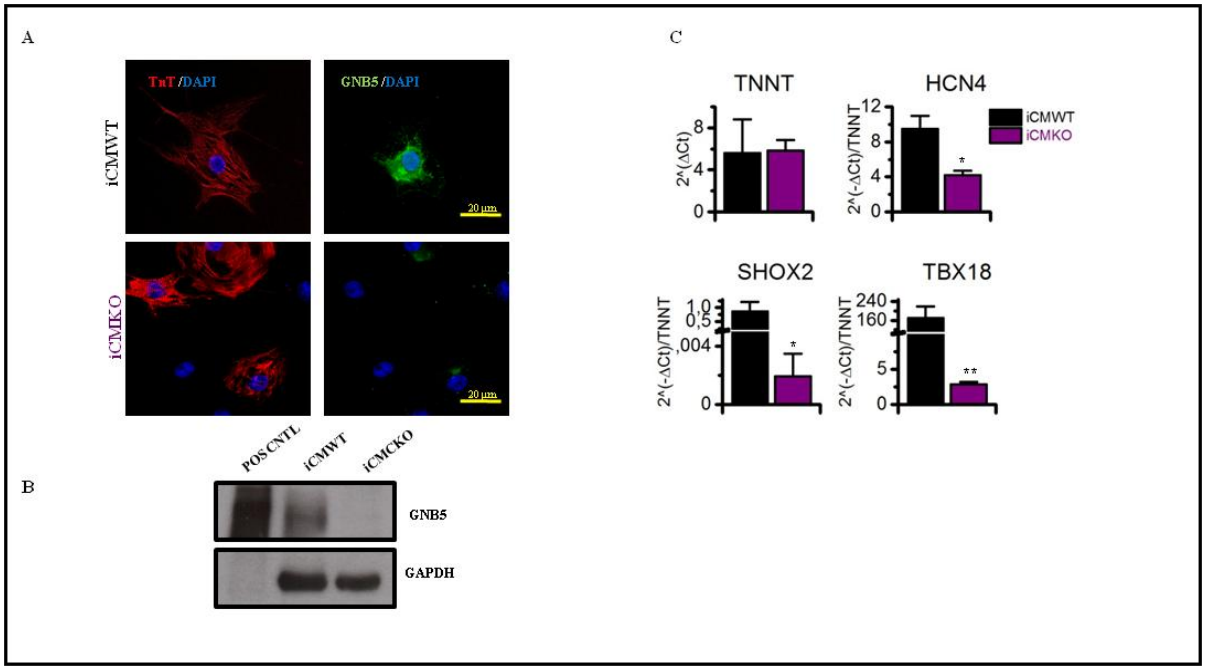


**Figure 14.** (A) Representative immunofluorescence images of iCM (induced cardyomyocites), stained with anti-cardiac TnT (red) and anti-GNB5 (green) antibodies, highlighting the lack of GNB5 expression in the iCMKO (knockout) line. (B) Absence was further validated by Western Blot analysis in iCMKO protein lysate. (C) iCMKO cells showed a decreased expression of three well-known markers of sinus node compared to iCMWT cells demonstrating an impairment in the normal development and function of this specific tissue, a condition compatible with a pathological bradycardia. Student's t-test (*:p-value< 0.01; **p-value< 0.001; ***p-value< 0.0001).

The derived differentiated cells with different genotypes were analysed by the patch-clamp to evaluate spontaneous action potential (AP) rate.

Representative spontaneous APs, recorded by patch-clamp analysis from spontaneously beating iCM at 30 days of differentiation, are shown (https://www.operapadrepio.it/media-genetics/icm_videos/ClusteriCMGNB5KO40X/video.html) for iCMWT (black) and iCMKO lines (purple) in Figure 15A. These electrophysiological preliminary results show that, on

average, iCMKO present a marked bradycardia (21.2±15.9 bpm, n=4) when compared to control cardiomyocytes (87.2±37.8 bpm, n=5), confirming, from a functional point of view, an impaired commitment of iCM towards the sinus node-like phenotype, compatible with expression data. Addition of carbachol (100 nM), a stable agonist of M2-muscarinic receptors, on spontaneously beating iCM causes an expected a small decrease of rate in iCMWT lines while it almost stopps the action potential firing of iCMKO. This effect that suggests a hypersensitivity to muscarinic receptor activation, is clearly visible by the representative AP traces shown in Figure 15B and in the mean data showing the percent decrease in rate. Interestingly and in agreement with the hypothesis of muscarinic hypersensitivity, application of either atropine, a muscarinic antagonist widely used in clinics, or Tertiapin-Q, a blocker of the GIRK channels, significantly increase the firing rate, partially rescuing the bradycardic phenotype associated with the GNB5 KO (Figure 15C). These preliminary data demonstrate that the lack of GNB5 cause an intrinsic cell bradycardia that is somewhat associated with a basal hyperactivation of the muscarinic signalling and with an alteration of ion channels in general.

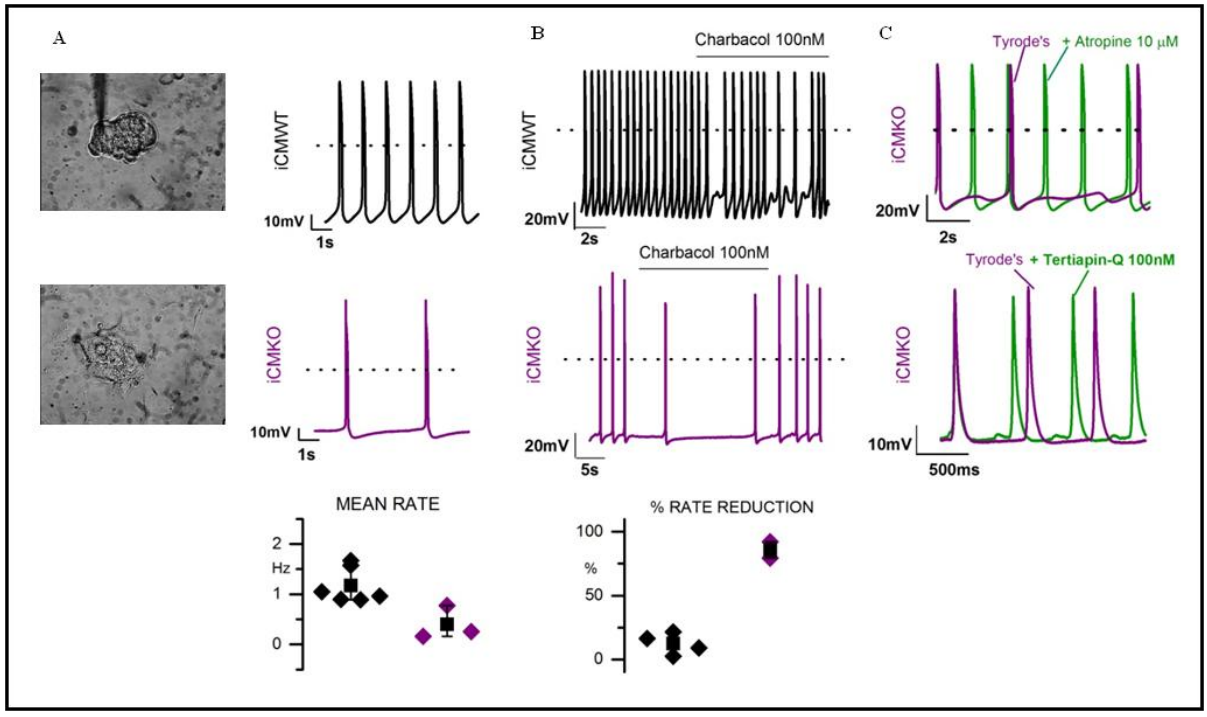


**Figure 15. (A)** Still images of video (https://www.operapadrepio.it/media-genetics/icm_videos/ClusteriCMGNB5KO40X/video.html) and representative action potential recordings from iCMWT and iCMKO (as indicated) demonstrating the intrinsic bradycardia associated with the lack of GNB5. iCMKO display a significantly higher sensitivity to the muscarinic agonist carbachol; however, both, the muscarinic antagonist atropine and the specific GIRK blocker Tertiapin-Q partially rescue the bradycardic phenotype of iCMKO. **(B)** iCMKO display a significantly higher sensitivity to the muscarinic agonist charbacol. **(C)** Both, the muscarinic antagonist atropine and the specific GIRK blocker Tertiapin-Q partially rescue the bradycardic phenotype of iCMKO.

## DISCUSSION

The GNB proteins are expressed in different and specific tissues and interact with many effectors to elicit a wide range of specific cellular responses. Therefore it is not surprising that variants that alter G-proteins functions compromise the appropriate cellular response, which is associated with aberration of physiological functions, and thus linked with a predisposition to develop human diseases. Consistently, in humans, variants in each of the five distinct G proteins beta-subunits (*GNB1-5*) cause rare genetic diseases.

We recently reported that germline LoF pathogenic variants in *GNB5* (*Gβ5*) cause a novel intellectual developmental disorder with cardiac arrhythmia (IDDCA) (Lodder et al., 2016). Since 2016, when the syndrome was identified, only 26 patients carrying 12 different genotypes have been described worldwide, including cases not yet published (Lodder et al., 2016; Shamseldin et al., 2016; Turkdogan et al., 2017; Malerba et al., 2018; Vernon et al., 2018).

Although the number of identified GNB5 pathogenetic variants is still small, there is a hot spot for GNB5 variants in exon 2 (50% of identified pathogenetic variants), encoding the first WD40 protein domain of the seven that characterize GNB5. The WD40 domain shows a beta-propeller structure that provides a stable scaffold for protein-protein interaction and is involved in a variety of cellular functions including signal transduction, autophagy, and apoptosis (Li and Roberts, 2001). Moreover, variants in WD40 domains are associated with an increasing number of human diseases (Laskowski et al., 2016). Of relevance, all the *GNB5* variants reported so far affect highly conserved amino acid residues and WD40 domains that was predicted to compromise GNB5 folding and/or stability (Shamseldin et al., 2016), its function and downstream regulated cellular processes, and the binding kinetics of RGS proteins (Lodder et al., 2016), leading to the clinical phenotype seen in the patients. Approximately 65% of *GNB5* variants found in our cohort are subject to frameshift or nonsense mutations that are predicted to generate premature termination codons (PTCs). PTC-bearing transcripts are often degraded by nonsense-mediated decay (NMD) resulting in loss-of-function (LoF) variant or null alleles. We experimentally showed that two transcripts from *GNB5* mutant alleles, reported as family A (Lodder et al., 2016) were subjected to mRNA degradation by NMD surveillance machinery.

Even though the paucity of patients reported, a genotype-phenotype correlation has emerged For instance, patients with missense variants are associated with a less severe/moderate phenotype characterized mainly by sinus node dysfunction in combination with mild intellectual disabilities without epileptic encephalopathy. In contrast, the majority of patients with *GNB5* homozygous null alleles are associated with severe intellectual disability, global

developmental delay including early infantile developmental and epileptic encephalopathy, hypotonia, as well as sinus node dysfunction (Lodder et al., 2016; Malerba et al., 2018; Vernon et al., 2018).

There are only two other patients, which are compound heterozygous for a missense and LoF GNB5 variant (Malerba et al., 2018; Vernon et al., 2018). Specifically, these two patients have the same p.(Asp74Glufs52*) LoF variant; but differ for the missense variant since the patient we recently described (Malerba et al., 2018) has the commonly reported p.(Ser81Leu) missense variant whereas the patient described in (Vernon et al., 2018) has a novel p.(Leu265Arg) missense variant. The latter might affect splicing and, although experimental assays are needed, it could cause a LoF, a type of variant more consistent with the phenotype seen in that patient. Features in common for these patients include psychomotor delay and sinus pauses.

Notably, our findings in *gnb5* knockout zebrafish model recapitulates some of the IDDCA clinical manifestations as it shows impaired swimming activity, abnormal ocular response, and sinus node dysfunction, due to a negative regulation of the cardiac GIRK channels (Lodder et al., 2016). Additionally, marked neurobehavioral abnormalities, including learning deficiencies, impaired gross motor coordination, abnormal gait (Zhang et al., 2011), defective visual adaptation (Krispel et al., 2003), and perturbed development and functioning of retinal bipolar cells (Rao et al., 2007) have been reported in *Gnb5* knockout mice, together with marked bradycardia (unpublished data). These evidences, together with the phenotype shared in individuals carrying GNB5 pathogenic variants, demonstrate the phenotypic consequences of heterotrimeric G-proteins deficiency and their key roles in neuronal and cardiac signalling.

This study arise with the goal to understand the (patho)physiological role of *GNB5* by using a combination of cutting-edge *in vitro* models, generating human cell types with the genetic and functional features of IDDCA syndrome. The use of patient-derived hiPSC offer an attractive experimental platform to model diseases, study the earliest stages of human development and the functional alterations of cells involved in the onset of specific traits of the pathology. (Takahashi et al., 2007).

The production of hiPSC-derived cardiomyocytes (hiPSC-CMs) are suitable model for human cardiovascular diseases since they carry the same genome as the patient they were generated from and, differently from animal models, they offer the physiological cell environment allowing to monitor the major parameters of heart function in terms of force, pacemaking activity, contraction and relaxation kinetics, as well as standard cardiac electrophysiology (Hansen et al., 2010; Mannhardt et al., 2016; Zhao and Bhattacharyya, 2018). Supporting this, to elucidate the physiological role of GNB5 in the pathogenesis of the cardiac phenotype

observed of IDDCA, we initially generated and characterized human induced pluripotent stem cells (hiPSC) from 4 IDDCA patients, 2 healthy parents and 4 unrelated controls. Moreover, to avoid any confounding genotype-intrinsic background variability of each IDDCA patient and control cell lines, we generate isogenic hiPSC line, in which we selectively knocked-down (KO) the *GNB5* expression via CRISPR-Cas9 system.

As first level of investigation, we chosen to use hiPSCKO and hiPSCWT to model, in *vitro*, the cardiac sinus node dysfunction as a hallmark of IDDCA, differentiating them in cardiomyocytes with pacemaker-like phenotype, by monolayer culture. Our preliminary results recorded by patch-clamp analysis showed that hiPSC-derived CMs from GNB5 null alleles (iCMKO) present a reduced spontaneous action potentials either with and without adding the agonist of $M_2$-muscarinic receptors (carbachol), resulting in a marked bradycardia when compared to control cardiomyocytes (iCMWT). This result suggests an hypersensitivity to muscarinic receptor activation.

Furthermore, in order to ameliorate and/or rescue the GNB5-associated cardiac phenotype, we tested some drugs through a fast perfusion system that allows the exchange of solutions around the cells in few seconds. Action potential properties have been recorded first in physiological solutions and during the perfusion of the selected drugs. Specifically, after application of either Atropine, a muscarinic ($M_2R$) antagonist widely used in clinics or Tertiapin-Q, a specific GIRK channels blocker, we showed a partially rescues of the bradycardic phenotype observed in iCMKO cells. Although additional studies will be required to dissect the precise mechanisms underlying the pathogenetic role of the GNB5 variants in IDDCA, these preliminary data, together with the previously data we published (Lodder et al., 2016) demonstrate that the lack of GNB5 cause an intrinsic cell bradycardia that is somewhat associated with a basal hyperactivation of the muscarinic signalling. Therefore our working-hypothesis is that inhibition of GIRK channels (by atropine, tertiapin-Q and other drugs), or modulation of any other channel/pathway that may induce the severe bradycardia, should be able to rescue the pathological phenotype linked to *GNB5* variants.

## CONCLUSIONS

This study extends the number of individuals carrying GNB5 pathogenic variants, and shows the phenotypic consequences of heterotrimeric G-proteins deficiency and their critical roles in cardiac manifestations. Additional patient studies will help us to more consistently predict phenotype based on their molecular results. Currently, therapeutic agents that modulate *GNB5* loss-of-function are not available. The integrated analysis proposed here, involving cellular

and electrophysiological analysis together with the future omics technologies carried out on different IDDCA relevant cell types, will provide a list of genes and/or pathways that are directly controlled by GNB5 and that may represent putative therapeutic targets.
Furthermore, the combination of cellular modeling and functional studies of cardiomyocytes demonstrate the potential drug-mediated therapeutic approach and provide new insights on the pathogenesis of the disease.

## FUTURE PERSPECTIVES

This study is currently on-going, it needs more time to deepen our understanding on how loss of *GNB5* activity affects crucial functional activities of cell lineages affected by the diseases.
For further data validation in a more specific disease-context we will use our *validation cohort*, including 4 IDDCA patients, 2 healthy parents and 4 unrelated controls of hiPSC-derived iCMs to evaluate the specific patients response to drugs administer. Moreover, since most IDDCA patients show epileptic encephalopathy/seizures and cognitive impairment, based on patient's symptoms and literature data, we are deriving both cortical excitatory and inhibitory (glutamatergic, and GABAergic) neurons from patient's hiPSC lines to unravel functional alterations associated with the *GNB5* LoF.
Although immediate benefits for patients are unpredictable, based on the functional alterations and through a drug screening, we will provide, indeed, some candidate compounds that will then be used as starting points for drug optimization programs for rescuing the heart- and brain-associated phenotypes linked to *GNB5* variants

## REFERENCES


Aguado C, Orlandi C, Fajardo-Serrano A, Gil-Minguez M, Martemyanov KA, Lujan R. 2016. Cellular and Subcellular Localization of the RGS7/Gbeta5/R7BP Complex in the Cerebellar Cortex. Front Neuroanat 10:114.

Anderson GR, Posokhova E, Martemyanov KA. 2009. The R7 RGS protein family: multi-subunit regulators of neuronal G protein signaling. Cell Biochem Biophys 54:33-46.

Arno G, Holder GE, Chakarova C, Kohl S, Pontikos N, Fiorentino A, Plagnol V, Cheetham ME, Hardcastle AJ, Webster AR, Michaelides M, Consortium UKIRD. 2016. Recessive Retinopathy Consequent on Mutant G-Protein beta Subunit 3 (GNB3). JAMA Ophthalmol 134:924-927.

Azzi M, Charest PG, Angers S, Rousseau G, Kohout T, Bouvier M, Pineyro G. 2003. Beta-arrestin-mediated activation of MAPK by inverse agonists reveals distinct active conformations for G protein-coupled receptors. Proc Natl Acad Sci U S A 100:11406-11411.

Barbuti A, Robinson RB. 2015. Stem cell-derived nodal-like cardiomyocytes as a novel pharmacologic tool: insights from sinoatrial node development and function. Pharmacol Rev 67:368-388.

Berman DM, Wilkie TM, Gilman AG. 1996. GAIP and RGS4 are GTPase-activating proteins for the Gi subfamily of G protein alpha subunits. Cell 86:445-452.

Bockaert J, Pin JP. 1999. Molecular tinkering of G protein-coupled receptors: an evolutionary success. EMBO J 18:1723-1729.

Cabrera-Vera TM, Vanhauwe J, Thomas TO, Medkova M, Preininger A, Mazzoni MR, Hamm HE. 2003. Insights into G protein structure, function, and regulation. Endocr Rev 24:765-781.

Chen CK, Burns ME, He W, Wensel TG, Baylor DA, Simon MI. 2000. Slowed recovery of rod photoresponse in mice lacking the GTPase accelerating protein RGS9-1. Nature 403:557-560.

Chen CK, Eversole-Cire P, Zhang H, Mancino V, Chen YJ, He W, Wensel TG, Simon MI. 2003. Instability of GGL domain-containing RGS proteins in mice lacking the G protein beta-subunit Gbeta5. Proc Natl Acad Sci U S A 100:6604-6609.

Chen IS, Tateyama M, Fukata Y, Uesugi M, Kubo Y. 2017. Ivermectin activates GIRK channels in a PIP2 -dependent, Gbetagamma -independent manner and an amino acid residue at the slide helix governs the activation. J Physiol 595:5895-5912.

Chung DW, Yoo KY, Hwang IK, Kim DW, Chung JY, Lee CH, Choi JH, Choi SY, Youn HY, Lee IS, Won MH. 2010. Systemic administration of lipopolysaccharide induces cyclooxygenase-2 immunoreactivity in endothelium and increases microglia in the mouse hippocampus. Cell Mol Neurobiol 30:531-541.

Clapham DE, Neer EJ. 1997. G protein beta gamma subunits. Annu Rev Pharmacol Toxicol 37:167-203.

Coskun V, Lombardo DM. 2016. Studying the pathophysiologic connection between cardiovascular and nervous systems using stem cells. J Neurosci Res 94:1499-1510.

D'Antonio M, D'Onorio De Meo P, Pallocca M, Picardi E, D'Erchia AM, Calogero RA, Castrignano T, Pesole G. 2015. RAP: RNA-Seq Analysis Pipeline, a new cloud-based NGS web application. BMC Genomics 16:S3.

Davies CH, Starkey SJ, Pozza MF, Collingridge GL. 1991. GABA autoreceptors regulate the induction of LTP. Nature 349:609-611.

De Vries L, Zheng B, Fischer T, Elenko E, Farquhar MG. 2000. The regulator of G protein signaling family. Annu Rev Pharmacol Toxicol 40:235-271.

Denayer T, Stohr T, Van Roy M. 2014. Animal models in translational medicine: Validation and prediction.

Devalla HD, Schwach V, Ford JW, Milnes JT, El-Haou S, Jackson C, Gkatzis K, Elliott DA, Chuva de Sousa Lopes SM, Mummery CL, Verkerk AO, Passier R. 2015. Atrial-like cardiomyocytes from human pluripotent stem cells are a robust preclinical model for assessing atrial-selective pharmacology. EMBO Mol Med 7:394-410.

DiFrancesco D, Ducouret P, Robinson RB. 1989. Muscarinic modulation of cardiac rate at low acetylcholine concentrations. Science 243:669-671.

DiFrancesco D. 2010. The role of the funny current in pacemaker activity. Circ Res 106:434-446.

Dupre DJ, Robitaille M, Rebois RV, Hebert TE. 2009. The role of Gbetagamma subunits in the organization, assembly, and function of GPCR signaling complexes. Annu Rev Pharmacol Toxicol 49:31-56.

Fajardo-Serrano A, Wydeven N, Young D, Watanabe M, Shigemoto R, Martemyanov KA, Wickman K, Lujan R. 2013. Association of Rgs7/Gbeta5 complexes with Girk channels and GABAB receptors in hippocampal CA1 pyramidal neurons. Hippocampus 23:1231-1245.

Fletcher JE, Lindorfer MA, DeFilippo JM, Yasuda H, Guilmard M, Garrison JC. 1998. The G protein beta5 subunit interacts selectively with the Gq alpha subunit. J Biol Chem 273:636-644.

Fredriksson R, Lagerstrom MC, Lundin LG, Schioth HB. 2003. The G-protein-coupled receptors in the human genome form five main families. Phylogenetic analysis, paralogon groups, and fingerprints. Mol Pharmacol 63:1256-1272.

Gautam N, Downes GB, Yan K, Kisselev O. 1998. The G-protein betagamma complex. Cell Signal 10:447-455.

Gilman AG. 1987. G proteins: transducers of receptor-generated signals. Annu Rev Biochem 56:615-649.

Gold SJ, Ni YG, Dohlman HG, Nestler EJ. 1997. Regulators of G-protein signaling (RGS) proteins: region-specific expression of nine subtypes in rat brain. J Neurosci 17:8024-8037.

Hansen A, Eder A, Bonstrup M, Flato M, Mewe M, Schaaf S, Aksehirlioglu B, Schwoerer AP, Uebeler J, Eschenhagen T. 2010. Development of a drug screening platform based on engineered heart tissue. Circ Res 107:35-44.

Hepler JR, Berman DM, Gilman AG, Kozasa T. 1997. RGS4 and GAIP are GTPase-activating proteins for Gq alpha and block activation of phospholipase C beta by gamma-thio-GTP-Gq alpha. Proc Natl Acad Sci U S A 94:428-432.

Hibino H, Inanobe A, Furutani K, Murakami S, Findlay I, Kurachi Y. 2010. Inwardly rectifying potassium channels: their structure, function, and physiological roles. Physiol Rev 90:291-366.

Hotta A, Yamanaka S. 2015. From Genomics to Gene Therapy: Induced Pluripotent Stem Cells Meet Genome Editing. Annu Rev Genet 49:47-70.

Hunt TW, Fields TA, Casey PJ, Peralta EG. 1996. RGS10 is a selective activator of G alpha i GTPase activity. Nature 383:175-177.

Jain BP, Pandey S. 2018. WD40 Repeat Proteins: Signalling Scaffold with Diverse Functions. Protein J 37:391-406.

Jara-Avaca M, Kempf H, Ruckert M, Robles-Diaz D, Franke A, de la Roche J, Fischer M, Malan D, Sasse P, Solodenko W, Drager G, Kirschning A, Martin U, Zweigerdt R. 2017. EBIO Does Not Induce Cardiomyogenesis in Human Pluripotent Stem Cells but Modulates Cardiac Subtype Enrichment by Lineage-Selective Survival. Stem Cell Reports 8:305-317.

Kamato D, Burch ML, Osman N, Zheng W, Little PJ. 2013. Therapeutic implications of endothelin and thrombin G-protein-coupled receptor transactivation of tyrosine and serine/threonine kinase cell surface receptors. J Pharm Pharmacol 65:465-473.

Khan SM, Sleno R, Gora S, Zylbergold P, Laverdure JP, Labbe JC, Miller GJ, Hebert TE. 2013. The expanding roles of Gbetagamma subunits in G protein-coupled receptor signaling and drug action. Pharmacol Rev 65:545-577.

Kozasa T, Jiang X, Hart MJ, Sternweis PM, Singer WD, Gilman AG, Bollag G, Sternweis PC. 1998. p115 RhoGEF, a GTPase activating protein for Galpha12 and Galpha13. Science 280:2109-2111.

Krishnan A, Mustafa A, Almen MS, Fredriksson R, Williams MJ, Schioth HB. 2015. Evolutionary hierarchy of vertebrate-like heterotrimeric G protein families. Mol Phylogenet Evol 91:27-40.

Krispel CM, Chen CK, Simon MI, Burns ME. 2003. Novel form of adaptation in mouse retinal rods speeds recovery of phototransduction. J Gen Physiol 122:703-712.

Kubo Y, Reuveny E, Slesinger PA, Jan YN, Jan LY. 1993. Primary structure and functional expression of a rat G-protein-coupled muscarinic potassium channel. Nature 364:802-806.

Kulkarni K, Xie X, Marron Fernandez de Velasco E, Anderson A, Martemyanov KA, Wickman K, Tolkacheva EG. 2018. Correction: The influences of the M2R-GIRK4-RGS6 dependent parasympathetic pathway on electrophysiological properties of the mouse heart. PLoS One 13:e0200553.

Lagerstrom MC, Schioth HB. 2008. Structural diversity of G protein-coupled receptors and significance for drug discovery. Nat Rev Drug Discov 7:339-357.

Laskowski RA, Tyagi N, Johnson D, Joss S, Kinning E, McWilliam C, Splitt M, Thornton JM, Firth HV, Wright CF. 2016. Integrating population variation and protein structural analysis to improve clinical interpretation of missense variation: application to the WD40 domain. Hum Mol Genet 25:927-935.

Lesage F, Duprat F, Fink M, Guillemare E, Coppola T, Lazdunski M, Hugnot JP. 1994. Cloning provides evidence for a family of inward rectifier and G-protein coupled K+ channels in the brain. FEBS Lett 353:37-42.

Li D, Roberts R. 2001. WD-repeat proteins: structure characteristics, biological function, and their involvement in human diseases. Cell Mol Life Sci 58:2085-2097.

Liang G, Zhang Y. 2013. Embryonic stem cell and induced pluripotent stem cell: an epigenetic perspective. Cell Res 23:49-69.

Lodder EM, De Nittis P, Koopman CD, Wiszniewski W, Moura de Souza CF, Lahrouchi N, Guex N, Napolioni V, Tessadori F, Beekman L, Nannenberg EA, Boualla L, Blom NA, de Graaff W, Kamermans M, Cocciadiferro D, Malerba N, Mandriani B, Akdemir ZHC, Fish RJ, Eldomery MK, Ratbi I, Wilde AAM, de Boer T, Simonds WF, Neerman-Arbez M, Sutton VR, Kok F, Lupski JR, Reymond A, Bezzina CR, Bakkers J, Merla G. 2016. GNB5 Mutations Cause an Autosomal-Recessive Multisystem Syndrome with Sinus Bradycardia and Cognitive Disability. Am J Hum Genet 99:704-710.

Lujan R, Ciruela F. 2012. GABAB receptors-associated proteins: potential drug targets in neurological disorders? Curr Drug Targets 13:129-144.

Lujan R, Marron Fernandez de Velasco E, Aguado C, Wickman K. 2014. New insights into the therapeutic potential of Girk channels. Trends Neurosci 37:20-29.

Luscher C, Slesinger PA. 2010. Emerging roles for G protein-gated inwardly rectifying potassium (GIRK) channels in health and disease. Nat Rev Neurosci 11:301-315.

Malerba N, Towner S, Keating K, Squeo GM, Wilson W, Merla G. 2018. A NGS-Targeted Autism/ID Panel Reveals Compound Heterozygous GNB5 Variants in a Novel Patient. Front Genet 9:626.

Mangoni ME, Nargeot J. 2008. Genesis and regulation of the heart automaticity. Physiol Rev 88:919-982.

Mannhardt I, Breckwoldt K, Letuffe-Breniere D, Schaaf S, Schulz H, Neuber C, Benzin A, Werner T, Eder A, Schulze T, Klampe B, Christ T, Hirt MN, Huebner N, Moretti A,

Eschenhagen T, Hansen A. 2016. Human Engineered Heart Tissue: Analysis of Contractile Force. Stem Cell Reports 7:29-42.
Martemyanov KA, Yoo PJ, Skiba NP, Arshavsky VY. 2005. R7BP, a novel neuronal protein interacting with RGS proteins of the R7 family. J Biol Chem 280:5133-5136.
McCudden CR, Hains MD, Kimple RJ, Siderovski DP, Willard FS. 2005. G-protein signaling: back to the future. Cell Mol Life Sci 62:551-577.
Morris AJ, Malbon CC. 1999. Physiological regulation of G protein-linked signaling. Physiol Rev 79:1373-1430.
Nakao R, Tanaka H, Takitani K, Kajiura M, Okamoto N, Kanbara Y, Tamai H. 2012. GNB3 C825T polymorphism is associated with postural tachycardia syndrome in children. Pediatr Int 54:829-837.
Neer EJ, Schmidt CJ, Nambudripad R, Smith TF. 1994. The ancient regulatory-protein family of WD-repeat proteins. Nature 371:297-300.
Neer EJ. 1995. Heterotrimeric G proteins: organizers of transmembrane signals. Cell 80:249-257.
Nikonov SS, Lyubarsky A, Fina ME, Nikonova ES, Sengupta A, Chinniah C, Ding XQ, Smith RG, Pugh EN, Jr., Vardi N, Dhingra A. 2013. Cones respond to light in the absence of transducin beta subunit. J Neurosci 33:5182-5194.
Noma A, Trautwein W. 1978. Relaxation of the ACh-induced potassium current in the rabbit sinoatrial node cell. Pflugers Arch 377:193-200.
Omole AE, Fakoya AOJ. 2018. Ten years of progress and promise of induced pluripotent stem cells: historical origins, characteristics, mechanisms, limitations, and potential applications. PeerJ 6:e4370.
Ostrovskaya O, Xie K, Masuho I, Fajardo-Serrano A, Lujan R, Wickman K, Martemyanov KA. 2014. RGS7/Gbeta5/R7BP complex regulates synaptic plasticity and memory by modulating hippocampal GABABR-GIRK signaling. Elife 3:e02053.
Pellegrino S, Zhang S, Garritsen A, Simonds WF. 1997. The coiled-coil region of the G protein beta subunit. Mutational analysis of Ggamma and effector interactions. J Biol Chem 272:25360-25366.
Petrovski S, Kury S, Myers CT, Anyane-Yeboa K, Cogne B, Bialer M, Xia F, Hemati P, Riviello J, Mehaffey M, Besnard T, Becraft E, Wadley A, Politi AR, Colombo S, Zhu X, Ren Z, Andrews I, Dudding-Byth T, Schneider AL, Wallace G, University of Washington Center for Mendelian G, Rosen AB, Schelley S, Enns GM, Corre P, Dalton J, Mercier S, Latypova X, Schmitt S, Guzman E, Moore C, Bier L, Heinzen EL, Karachunski P, Shur N, Grebe T, Basinger A, Nguyen JM, Bezieau S, Wierenga K, Bernstein JA, Scheffer IE, Rosenfeld JA, Mefford HC, Isidor B, Goldstein DB. 2016. Germline De Novo Mutations in GNB1 Cause Severe Neurodevelopmental Disability, Hypotonia, and Seizures. Am J Hum Genet.
Pierce KL, Premont RT, Lefkowitz RJ. 2002. Seven-transmembrane receptors. Nat Rev Mol Cell Biol 3:639-650.
Posokhova E, Wydeven N, Allen KL, Wickman K, Martemyanov KA. 2010. RGS6/Gbeta5 complex accelerates IKACh gating kinetics in atrial myocytes and modulates parasympathetic regulation of heart rate. Circ Res 107:1350-1354.
Rajagopal S, Rajagopal K, Lefkowitz RJ. 2010. Teaching old receptors new tricks: biasing seven-transmembrane receptors. Nat Rev Drug Discov 9:373-386.
Rao A, Dallman R, Henderson S, Chen CK. 2007. Gbeta5 is required for normal light responses and morphology of retinal ON-bipolar cells. J Neurosci 27:14199-14204.
Robishaw JD, Berlot CH. 2004. Translating G protein subunit diversity into functional specificity. Curr Opin Cell Biol 16:206-209.
Rosenbaum DM, Rasmussen SG, Kobilka BK. 2009. The structure and function of G-protein-coupled receptors. Nature 459:356-363.

Ross EM, Wilkie TM. 2000. GTPase-activating proteins for heterotrimeric G proteins: regulators of G protein signaling (RGS) and RGS-like proteins. Annu Rev Biochem 69:795-827.

Schuler V, Luscher C, Blanchet C, Klix N, Sansig G, Klebs K, Schmutz M, Heid J, Gentry C, Urban L, Fox A, Spooren W, Jaton AL, Vigouret J, Pozza M, Kelly PH, Mosbacher J, Froestl W, Kaslin E, Korn R, Bischoff S, Kaupmann K, van der Putten H, Bettler B. 2001. Epilepsy, hyperalgesia, impaired memory, and loss of pre- and postsynaptic GABA(B) responses in mice lacking GABA(B(1)). Neuron 31:47-58.

Shamseldin HE, Masuho I, Alenizi A, Alyamani S, Patil DN, Ibrahim N, Martemyanov KA, Alkuraya FS. 2016. GNB5 mutation causes a novel neuropsychiatric disorder featuring attention deficit hyperactivity disorder, severely impaired language development and normal cognition. Genome Biol 17:195.

Simonds WF, Zhang JH. 2000. New dimensions in G protein signalling: G beta 5 and the RGS proteins. Pharm Acta Helv 74:333-336.

Slepak VZ. 2009. Structure, function, and localization of Gbeta5-RGS complexes. Prog Mol Biol Transl Sci 86:157-203.

Smrcka AV. 2008. G protein betagamma subunits: central mediators of G protein-coupled receptor signaling. Cell Mol Life Sci 65:2191-2214.

Soldner F, Jaenisch R. 2018. Stem Cells, Genome Editing, and the Path to Translational Medicine. Cell 175:615-632.

Sondek J, Bohm A, Lambright DG, Hamm HE, Sigler PB. 1996. Crystal structure of a G-protein beta gamma dimer at 2.1A resolution. Nature 379:369-374.

Sondek J, Siderovski DP. 2001. Ggamma-like (GGL) domains: new frontiers in G-protein signaling and beta-propeller scaffolding. Biochem Pharmacol 61:1329-1337.

Soong BW, Huang YH, Tsai PC, Huang CC, Pan HC, Lu YC, Chien HJ, Liu TT, Chang MH, Lin KP, Tu PH, Kao LS, Lee YC. 2013. Exome sequencing identifies GNB4 mutations as a cause of dominant intermediate Charcot-Marie-Tooth disease. Am J Hum Genet 92:422-430.

Stallmeyer B, Kuss J, Kotthoff S, Zumhagen S, Vowinkel K, Rinne S, Matschke LA, Friedrich C, Schulze-Bahr E, Rust S, Seebohm G, Decher N, Schulze-Bahr E. 2017. A Mutation in the G-Protein Gene GNB2 Causes Familial Sinus Node and Atrioventricular Conduction Dysfunction. Circ Res 120:e33-e44.

Takahashi K, Yamanaka S. 2006. Induction of pluripotent stem cells from mouse embryonic and adult fibroblast cultures by defined factors. Cell 126:663-676.

Takahashi K, Tanabe K, Ohnuki M, Narita M, Ichisaka T, Tomoda K, Yamanaka S. 2007. Induction of pluripotent stem cells from adult human fibroblasts by defined factors. Cell 131:861-872.

Tayou J, Wang Q, Jang GF, Pronin AN, Orlandi C, Martemyanov KA, Crabb JW, Slepak VZ. 2016. Regulator of G Protein Signaling 7 (RGS7) Can Exist in a Homo-oligomeric Form That Is Regulated by Galphao and R7-binding Protein. J Biol Chem 291:9133-9147.

Trivellin G, Daly AF, Faucz FR, Yuan B, Rostomyan L, Larco DO, Schernthaner-Reiter MH, Szarek E, Leal LF, Caberg JH, Castermans E, Villa C, Dimopoulos A, Chittiboina P, Xekouki P, Shah N, Metzger D, Lysy PA, Ferrante E, Strebkova N, Mazerkina N, Zatelli MC, Lodish M, Horvath A, de Alexandre RB, Manning AD, Levy I, Keil MF, Sierra Mde L, Palmeira L, Coppieters W, Georges M, Naves LA, Jamar M, Bours V, Wu TJ, Choong CS, Bertherat J, Chanson P, Kamenicky P, Farrell WE, Barlier A, Quezado M, Bjelobaba I, Stojilkovic SS, Wess J, Costanzi S, Liu P, Lupski JR, Beckers A, Stratakis CA. 2014. Gigantism and acromegaly due to Xq26 microduplications and GPR101 mutation. N Engl J Med 371:2363-2374.

Trivellin G, Bjelobaba I, Daly AF, Larco DO, Palmeira L, Faucz FR, Thiry A, Leal LF, Rostomyan L, Quezado M, Schernthaner-Reiter MH, Janjic MM, Villa C, Wu TJ,

Stojilkovic SS, Beckers A, Feldman B, Stratakis CA. 2016. Characterization of GPR101 transcript structure and expression patterns. J Mol Endocrinol 57:97-111.
Tummala H, Ali M, Getty P, Hocking PM, Burt DW, Inglehearn CF, Lester DH. 2006. Mutation in the guanine nucleotide-binding protein beta-3 causes retinal degeneration and embryonic mortality in chickens. Invest Ophthalmol Vis Sci 47:4714-4718.
Turkdogan D, Usluer S, Akalin F, Agyuz U, Aslan ES. 2017. Familial early infantile epileptic encephalopathy and cardiac conduction disorder: A rare cause of SUDEP in infancy. Seizure 50:171-172.
Ulrich D, Bettler B. 2007. GABA(B) receptors: synaptic functions and mechanisms of diversity. Curr Opin Neurobiol 17:298-303.
Vernon H, Cohen J, De Nittis P, Fatemi A, McClellan R, Goldstein A, Malerba N, Guex N, Reymond A, Merla G. 2018. Intellectual developmental disorder with cardiac arrhythmia syndrome in a child with compound heterozygous GNB5 variants. Clin Genet 93:1254-1256.
Vilardaga JP, Agnati LF, Fuxe K, Ciruela F. 2010. G-protein-coupled receptor heteromer dynamics. J Cell Sci 123:4215-4220.
Vincent A, Audo I, Tavares E, Maynes JT, Tumber A, Wright T, Li S, Michiels C, Consortium GNB, Condroyer C, MacDonald H, Verdet R, Sahel JA, Hamel CP, Zeitz C, Heon E. 2016. Biallelic Mutations in GNB3 Cause a Unique Form of Autosomal-Recessive Congenital Stationary Night Blindness. Am J Hum Genet.
Watson AJ, Katz A, Simon MI. 1994. A fifth member of the mammalian G-protein beta-subunit family. Expression in brain and activation of the beta 2 isotype of phospholipase C. J Biol Chem 269:22150-22156.
Watson AJ, Aragay AM, Slepak VZ, Simon MI. 1996. A novel form of the G protein beta subunit Gbeta5 is specifically expressed in the vertebrate retina. J Biol Chem 271:28154-28160.
Xie K, Allen KL, Kourrich S, Colon-Saez J, Thomas MJ, Wickman K, Martemyanov KA. 2010. Gbeta5 recruits R7 RGS proteins to GIRK channels to regulate the timing of neuronal inhibitory signaling. Nat Neurosci 13:661-663.
Yakubovich D, Berlin S, Kahanovitch U, Rubinstein M, Farhy-Tselnicker I, Styr B, Keren-Raifman T, Dessauer CW, Dascal N. 2015. A Quantitative Model of the GIRK1/2 Channel Reveals That Its Basal and Evoked Activities Are Controlled by Unequal Stoichiometry of Galpha and Gbetagamma. PLoS Comput Biol 11:e1004598.
Yang J, Huang J, Maity B, Gao Z, Lorca RA, Gudmundsson H, Li J, Stewart A, Swaminathan PD, Ibeawuchi SR, Shepherd A, Chen CK, Kutschke W, Mohler PJ, Mohapatra DP, Anderson ME, Fisher RA. 2010. RGS6, a modulator of parasympathetic activation in heart. Circ Res 107:1345-1349.
Ye Y, Sun Z, Guo A, Song LS, Grobe JL, Chen S. 2014. Ablation of the GNB3 gene in mice does not affect body weight, metabolism or blood pressure, but causes bradycardia. Cell Signal 26:2514-2520.
Yoshikawa DM, Hatwar M, Smrcka AV. 2000. G protein beta 5 subunit interactions with alpha subunits and effectors. Biochemistry 39:11340-11347.
Yoshioka N, Gros E, Li HR, Kumar S, Deacon DC, Maron C, Muotri AR, Chi NC, Fu XD, Yu BD, Dowdy SF. 2013. Efficient generation of human iPSCs by a synthetic self-replicative RNA. Cell Stem Cell 13:246-254.
Zhang JH, Pandey M, Seigneur EM, Panicker LM, Koo L, Schwartz OM, Chen W, Chen CK, Simonds WF. 2011. Knockout of G protein beta5 impairs brain development and causes multiple neurologic abnormalities in mice. J Neurochem 119:544-554.
Zhang L, Zhang H, Sun K, Song Y, Hui R, Huang X. 2005. The 825C/T polymorphism of G-protein beta3 subunit gene and risk of ischaemic stroke. J Hum Hypertens 19:709-714.

Zhao J, Deng Y, Jiang Z, Qing H. 2016. G Protein-Coupled Receptors (GPCRs) in Alzheimer's Disease: A Focus on BACE1 Related GPCRs. Front Aging Neurosci 8:58.

Zhao X, Bhattacharyya A. 2018. Human Models Are Needed for Studying Human Neurodevelopmental Disorders. Am J Hum Genet 103:829-857.

Zhou H, Chisari M, Raehal KM, Kaltenbronn KM, Bohn LM, Mennerick SJ, Blumer KJ. 2012. GIRK channel modulation by assembly with allosterically regulated RGS proteins. Proc Natl Acad Sci U S A 109:19977-19982.